International Journal of Heat and Fluid Flow 66 (2017) 43–59

Contents lists available at ScienceDirect

International Journal of Heat and Fluid Flow

journal homepage: www.elsevier.com/locate/ijhff

Flow analysis of square-back simplified vehicles in platoon

Charles-Henri Bruneau[a,b,*], Khodor Khadra[a], Iraj Mortazavi[c]

[a] University of Bordeaux, CNRS IMB UMR 5251, 351, cours de la Libération, F-33405 Talence, France
[b] INRIA Bordeaux-Sud-Ouest MEMPHIS, France
[c] M2N EA-7340, Conservatoire National des Arts et Métiers, 2 Rue Conté, F-75003 Paris, France

ARTICLE INFO

Article history:
Received 30 September 2016
Revised 3 May 2017
Accepted 14 May 2017

MSC:
00-01
99-00

Keywords:
Square back Ahmed body
European tractor-trailer
Ground vehicles platooning
Aerodynamics
Direct numerical simulation
Penalization method

ABSTRACT

The aim of this work is to study the platooning of square-back vehicles on top of a road. When two or three bodies are following each other with a short distance between them, the presence of the preceding body changes significantly the pressure force in front of the following one as a weak flow is present in between. The preceding body plays the role of a buckler and so the following body has to face completely different flow conditions. Therefore the drag coefficient of the following bodies can be drastically reduced as shown on the results. But the reduction is strongly linked to the distance between the bodies and the differences are significant. The numerical simulations are performed around simplified vehicles, namely the square back Ahmed body and the simplified European tractor-trailer geometry. The results are also linked to the shape of the bodies.

1. Introduction

Saving energy has become one of the main challenges of human beings today. Among energy consumers, transportation represents a significant part, in particular ground transportation. Flow control is a way to reduce the consumption but another way is platooning. The idea is to take benefit of the following vehicle to reduce the drag coefficient and thus to save energy. Many researchers try to improve inter vehicular communications. The goal is to have trucks autonomously following their leaders to form a road train in order to improve traffic flow efficiency and to reduce fuel consumption. Since the 1980s inter vehicular communications have been developed as can be seen in Segata et al. (2015); Sommer and Dressler (2014); van Arem et al. (2006) and references therein. In parallel some research studies have been performed on the flow dynamics to quantify the impact on the drag coefficient. The researches concern more stochastic optimization (Caltagirone et al., 2015; Farokhi and Johansson, 2014) than aerodynamics (Caltagirone et al., 2015; Bruneau et al., 2013; Uystepruyst and Krajnović, 2013). In Kavathekar and Chen (2011) the authors describe precisely what is vehicle platooning and provide a summary of the literature published between 1994 and 2010. Driving in a platoon has generally been considered to offer a reduction in aerodynamic drag for all the vehicles. Many experiments and numerical simulations have been performed, specially with Ahmed bodies with a rear slant angle and for different inter-vehicle distances (Pagliarella, 2009; Pagliarella and Watkins, 2016; Watkins and Vino, 2008). In Mirzaei and Krajnović (2016); Pagliarella (2009); Pagliarella and Watkins (2016); Watkins and Vino (2008), for the case of two Ahmed bodies with a critical slant angle, a drag increase was observed for the follower compared to the drag value of a single body in isolation. Finally, in Frahadi and Sedighi (2008) the authors studied numerically the flow behavior around two tandem cubes depending on their distance. They explored the cavity-like effects for such a configuration. That is why in this paper only square-back bodies close to tractor-trailers or heavy-duty vehicles are considered.

Concerning heavy-duty vehicles platooning, many experimental studies have been made comparing to a few numerical simulations. They show that the best choice with respect to a heavier or lighter lead vehicle depends on the desired time gap. For example, a maximum fuel reduction of 4.7% to 7.7% depending on the time gap, at a set speed of 70 km/h, can be obtained with two identical trucks (Alam et al., 2010). A few numerical simulations on heavy-duty vehicules were conducted, the separation distance was varied in order to determine how the drag reduction behaves with respect to

* Corresponding author.
E-mail addresses: charles-henri.bruneau@math.u-bordeaux.fr (C.-H. Bruneau), Khodor.Khadra@math.u-bordeaux.fr (K. Khadra), iraj.mortazavi@cnam.fr (I. Mortazavi).

http://dx.doi.org/10.1016/j.ijheatfluidflow.2017.05.008
0142-727X/

the separation distance. The simulation data show that the percent drag reduction increases with decreasing separation distance. For two trucks (Humphreys and Bevly, 2016), and a twenty feet separation distance, the front truck and the rear truck have respectively a drag reduction close to 13% and 34%. In the case of three heavy-duty vehicles resulting drag coefficients are shown in Watts (2015) as a percentage of single vehicle drag according to the distance between the vehicles. For a twenty feet separation distance, the front vehicule, the middle one and the rear one have respectively a drag reduction close to 13%, 48% and 40%.

In this work the flow around one single, two or three following simplified square-back ground vehicles called Ahmed body (Ahmed et al., 1984) or European tractor-trailer geometry is simulated. The study is performed using direct numerical simulations to achieve an accurate benchmarking with a very fine flow resolution. Therefore, Reynolds number values are low compared to road configurations but permit to achieve precise flow trends in various platooning cases. The method has been validated for square back Ahmed bodies (Bruneau et al., 2013). In order to study the influence of the distance between the bodies to the flow characteristics, the distance d between the bodies is set to 20%, 50% and 100% of the length of Ahmed body. The shortest distance is close to the best results obtained for inter vehicular communications (Segata et al., 2015). These three distances allow to observe the influence of a close body to the development of the wake of the preceding one and to quantify the impact on the drag coefficient. The influence of the preceding body to the flow around the following body is also explored. As expected the first body plays the role of a buckler and thus the second body does not face at all the same flow conditions at infinity than the first one. Now it is well known that a large part of the drag coefficient around the bodies is due to the pressure forces on the front and at the back walls (Bruneau et al., 2014; Brunn et al., 2007; Krajnović and Davidson, 2003). Therefore, in this case, the pressure forces are drastically reduced and so is the drag coefficient. According to the distance between the bodies, the flow inside the gap between the bodies changes as the wake of the preceding body cannot fully develop. Consequently the pressure forces change and thus the drag coefficient of both bodies. Indeed, when the wake is compressed by the following body, the pressure increases, the pressure force at the back of the preceding one decreases and the drag coefficient also decreases. We shall see that platooning can decrease significantly the drag coefficient of the whole train. Some numerical experiments on a simplified European tractor-trailer geometry confirm the benefit of platooning in a more realistic configuration.

This paper is organized in four sections in addition to this introduction. The first one is devoted to the modeling and numerical simulations. The second one concerns the numerical results around one, two or three Ahmed bodies in two or three dimensions. In the third section the flow around the simplified European tractor-trailer geometry (SETTG) is presented. At the end some conclusions are provided.

2. Modeling and numerical simulations

In this section, the method used to simulate the flow past full scale Ahmed bodies on top of a road using Cartesian grids is presented. To compute the flow around solid bodies an immersed boundary model is used, namely the penalized Navier–Stokes equations for the velocity and pressure (U, p) as unknowns (Angot et al., 1999). The non dimensional form based on the far field velocity of the flow U_∞ and the height H of Ahmed body, these equations read:

$$\partial_t U + (U\cdot\nabla)U - \frac{1}{Re}\Delta U + \frac{U}{K} + \nabla p = 0 \;\; in\; \Omega_T = \Omega\times(0,T) \quad (1)$$

$$\nabla U = 0 \;\; in\; \Omega_T \quad (2)$$

where $Re = \frac{|U_\infty|H}{\nu}$ is the non dimensional Reynolds number associated to the kinematic viscosity of the fluid ν, $K = \frac{k|U_\infty|}{\nu\Phi H} = \frac{kRe}{\Phi H^2}$ is the non dimensional coefficient of permeability of the medium representing the bodies with k the intrinsic permeability and Φ the porosity of the medium, Ω is the full domain including the solid bodies and T is the simulation time. In the fluid domain the permeability coefficient goes to infinity, the penalization term vanishes and we solve the genuine non dimensional Navier-Stokes equations. In the solid body the permeability coefficient goes to zero, so U/K is large and dominate other velocity terms that become negligible. It has been shown in Angot et al. (1999) that solving these equations corresponds to solve Darcy's law in the solid parts and that the velocity is proportional to K. For numerical simulations we set $K = 10^{16}$ in the fluid and $K = 10^{-8}$ in the solid bodies. In the non dimensional form of the equations the time is $t = t_r \mid U_\infty \mid /H$ and the pressure is $p = p_r/(\rho_r \mid U_\infty \mid^2)$ where the subscript r stands for the real values.

The Eqs. (1) and (2) above are associated to an initial datum $(X = (x, y, z)$ in 3D):

$U(X, 0) = U_0(X)$ in Ω and the following boundary conditions:

$U = U_\infty = (u_\infty, 0, 0) = (1, 0, 0)$ at the entrance section and on the road;

$\partial_n U = 0$ on the longitudinal far field boundaries;

$\sigma(U, p)n + \frac{1}{2}(U\cdot n)^-(U - U_{ref}) = \sigma(U_{ref}, p_{ref})n$ on the exit downstream boundary to convey properly the vortices through the artificial frontiers (Bruneau, 2000), where $\sigma(U, p) = 1/Re(\nabla U + \nabla U^t) - pI$ is the stress tensor, n is the unit normal pointing outside of the domain and the notation $a = a^+ - a^-$ is used.

Then a simulation is performed using a second-order Gear scheme in time with explicit treatment of the convection term. All the linear terms are treated implicitly and discretized via a second-order centered finite differences scheme. The CFL condition related to the convection term requires a time step of the order of magnitude of the space step as U is of order one. A third-order finite differences upwind scheme is used for the space discretization of the convection terms (Bruneau and Saad, 2006). The efficiency of the resolution is obtained by a multigrid procedure using a cell-by-cell Gauss–Seidel smoother. For each cell in 3D, it consists in reversing the 7×7 matrix:

$$\begin{pmatrix} a_{11} & 0 & 0 & 0 & 0 & 0 & \frac{1}{\delta x} \\ 0 & a_{22} & 0 & 0 & 0 & 0 & -\frac{1}{\delta x} \\ 0 & 0 & a_{33} & 0 & 0 & 0 & \frac{1}{\delta y} \\ 0 & 0 & 0 & a_{44} & 0 & 0 & -\frac{1}{\delta y} \\ 0 & 0 & 0 & 0 & a_{55} & 0 & \frac{1}{\delta z} \\ 0 & 0 & 0 & 0 & 0 & a_{66} & -\frac{1}{\delta z} \\ -\frac{1}{\delta x} & \frac{1}{\delta x} & -\frac{1}{\delta y} & \frac{1}{\delta y} & -\frac{1}{\delta z} & \frac{1}{\delta z} & 0 \end{pmatrix} \times \begin{pmatrix} u_{i-\frac{1}{2},j,k} \\ u_{i+\frac{1}{2},j,k} \\ v_{i,j-\frac{1}{2},k} \\ v_{i,j+\frac{1}{2},k} \\ w_{i,j,k-\frac{1}{2}} \\ w_{i,j,k+\frac{1}{2}} \\ p_{i,j,k} \end{pmatrix} = \begin{pmatrix} b_1 \\ b_2 \\ b_3 \\ b_4 \\ b_5 \\ b_6 \\ b_7 \end{pmatrix} \quad (3)$$

with $(a_{ii})_{1\le i\le 6}$ the diagonal composed of the time term, the diagonal of the linear diffusion terms and the penalization term, and $(b_i)_{1\le i\le 7}$ the second member made of all the remaining terms including the non-linear convection terms and the second member of the equation if any.

Several test cases are considered in this work. The first test case is to compute the flow over a single square back Ahmed body on

Table 1
Grid convergence for the flow around one single body on top of a road in a short domain $\Omega = (0, 10H) \times (0, 6H) \times (0, 6H)$.

3D simulation	G6	G7	G8	G9
Number of cells	11,796,480	94,371,840	754,974,720	6,039,797,760
C_D	0.522	0.487	0.467	0.463

top of a road. Then the platooning of two or three bodies is considered in two- and three-dimensions. Let H be the height, $W = 1.3507H$ and $L = 3.625H$ be respectively the width and the length of the square back Ahmed bodies, the distance d between the bodies is set to $d = 0.2L$, $d = 0.5L$ and $d = L$ to study the variation of the characteristics of the flow with respect to d. The simulations are performed in a computational domain $\Omega = (0, 20H) \times (0, 4H)$ in two-dimensions or $\Omega = (0, 20H) \times (0, 6H) \times (0, 6H)$ in three-dimensions with the bodies located at the distance $0.17H$ from the road. For the computation over three bodies the domain is extended to $24H$ in the x-direction with $d = 0.2L$ and $d = 0.5L$ and to $28H$ in the x-direction with $d = L$.

The cpu time is reduced using an efficient MPI parallelism (Bruneau and Khadra, 2016). The main difficulties are linked to the multigrid solver, on the one hand because of the cell-by-cell Gauss–Seidel smoother and not Jacobi smoother and, on the other hand due to the multigrid itself that uses very coarse grids that cannot be computed in parallel. Nevertheless the computational code can run on 384 cores in 3D with a strong scalability close to one (Bruneau and Khadra, 2016).

The results are presented at $Re = 15,000$ based on the body height H for all the test cases. This value is far to the real value as it corresponds to a velocity around one meter per second for Ahmed body to compare to a real value around 30 m per second. To insure the reliability of the results, the simulations are performed on four uniform meshes where grid convergence is reached on the drag coefficient (see Table 1). The values obtained here are about 25% higher than the value obtained in the experiments or numerical simulations with turbulence models at high Reynolds number. This is due to the low value of Re and the present DNS method has already been validated in previous works (Bruneau et al., 2013). The simulation for the grid convergence are performed around one single body in a short domain $\Omega = (0, 10H) \times (0, 6H) \times (0, 6H)$. The value obtained on the $G8$ grid and on the $G9$ grid are very close and thus the simulations will be performed on $G8$ in the following sections. On the domain $\Omega = (0, 20H) \times (0, 6H) \times (0, 6H)$ the grid $G8$ will have $2,560 \times 768 \times 768 = 1,509,949,440$ cells and 6,044,319,744 unknowns for the velocity and the pressure on staggered grids. The numerical simulations use a time step $\delta t = 10^{-3}$ in order to take into account the Kolmogorov time scale for the chosen low Reynolds number. In addition the simulation time will be large enough for the flow crosses the domain more than twice in order to get realistic mean flows.

The physical quantities are computed using either a direct computation or the penalization term. Indeed the drag and lift forces are given by:

$$F_D = -\int_{body} \partial_x p \, dX + \int_{body} \frac{1}{Re} \Delta u \, dX \approx \int_{body} \frac{u}{K} \, dX$$

$$F_L = -\int_{body} \partial_z p \, dX + \int_{body} \frac{1}{Re} \Delta w \, dX \approx \int_{body} \frac{w}{K} \, dX.$$

Then the drag coefficient C_D and the lift coefficient C_L are computed as usual:

$$C_D = 2F_D/S, \quad C_L = 2F_L/S,$$

where S is the cross section of the body. In two-dimensions $S = H$ and in three-dimensions $S = WH$. The results on the drag coefficient are very close with the two computations $G8$ and $G9$. The drag coefficient as well as the pressure forces in the front p_f and at the back p_b of the bodies are presented throughout the paper.

3. Numerical results with Ahmed body

3.1. Platooning on top of a road in two dimensions

In this section we explore the flow around one single or two Ahmed bodies following each other on top of a road. The simulations are performed in two-dimensions on a $2,560 \times 768$ grid at Reynolds number $Re = 15,000$. In Fig. 1 are represented the vorticity field and the pressure contours for one single body. Throughout the paper the red color stands for the negative vorticity and the blue color stands for the positive vorticity. It shows clearly that there is a long wake with a strong pressure well behind the body. Consequently both pressure forces in front p_f and at the back p_b are at a high level. They are in fact responsible of 95% of the drag coefficient. The history in Fig. 2 shows that the pressure force at the back is slightly higher than in front and that the drag coefficient is strongly linked to p_b. For instance at time 40, despite the pressure force in front is very high, the drag coefficient is quite low. Elsewhere the drag coefficient follows the variation of p_b. So, it is obvious that the presence of another body in the wake will change the pressure force p_b at the back of the preceding one and consequently will change the drag coefficient. Let us point out to the reader that the values of the drag coefficient correspond to both a low Reynolds number and the two-dimensions. What is considered in this paper are not the values themselves but their variation with platooning.

The main question is to know what is the best distance that insures a significant reduction of the drag coefficient for both bodies. We have decided to test three distances between the two vehicles $d = 0.2L = 0.725H$, $d = 0.5L = 1.8125H$ and $d = L = 3.625H$. The smallest distance corresponds to the best results obtained using inter vehicular communications (Segata et al., 2015). The results are computed in the same domain with the same grid than before. Fig. 3 shows again the vorticity field and the pressure contours for $d = 0.2L$. At this short distance the flow cannot develop in the gap between the two bodies that looks like the gap between trailers and behave as a cavity, the flow being dominated by a single vortex. As shown in Fig. 4, this time the pressure force at the back is much lower than the pressure force in front but the drag coefficient is still strongly linked to it. Table 2 even shows that the mean value is slightly negative. That means that the second body is so close that the pressure increases drastically in this cavity and pushes the first body. Consequently the drag coefficient is reduced by 64%. For the second body, as expected the pressure force in front is strongly reduced but also the pressure at the back. Indeed due to this lack of pressure in front of the second body, the wake is significantly shorter than for a single body as shown by the mean pressure contours in Figs. 1 and 4. Thus the pressure well is less deep. The conjunction of the two phenomena yields a drag reduction of 49% (see Table 2).

Now we increase the distance up to $d = 0.5L$. The vorticity field and the pressure contours are shown in Fig. 6. They show that for this distance the flow is developing inside the gap between the two vehicles. So there is a pressure well at the back of the first body and the pressure force is higher than before. Nevertheless the drag coefficient is reduced by 25%, which is much less than for $d = 0.2L$. Due to the pressure well at the back of the first body there is a tremendous decrease of the pressure force in front of the second body that is now slightly negative as shown in Table 2. That means that the second body is sucked by the first body. This phenomenon is well-known by the F1 pilots. In addition it implies also a reduction of the wake and both reductions induce a decrease

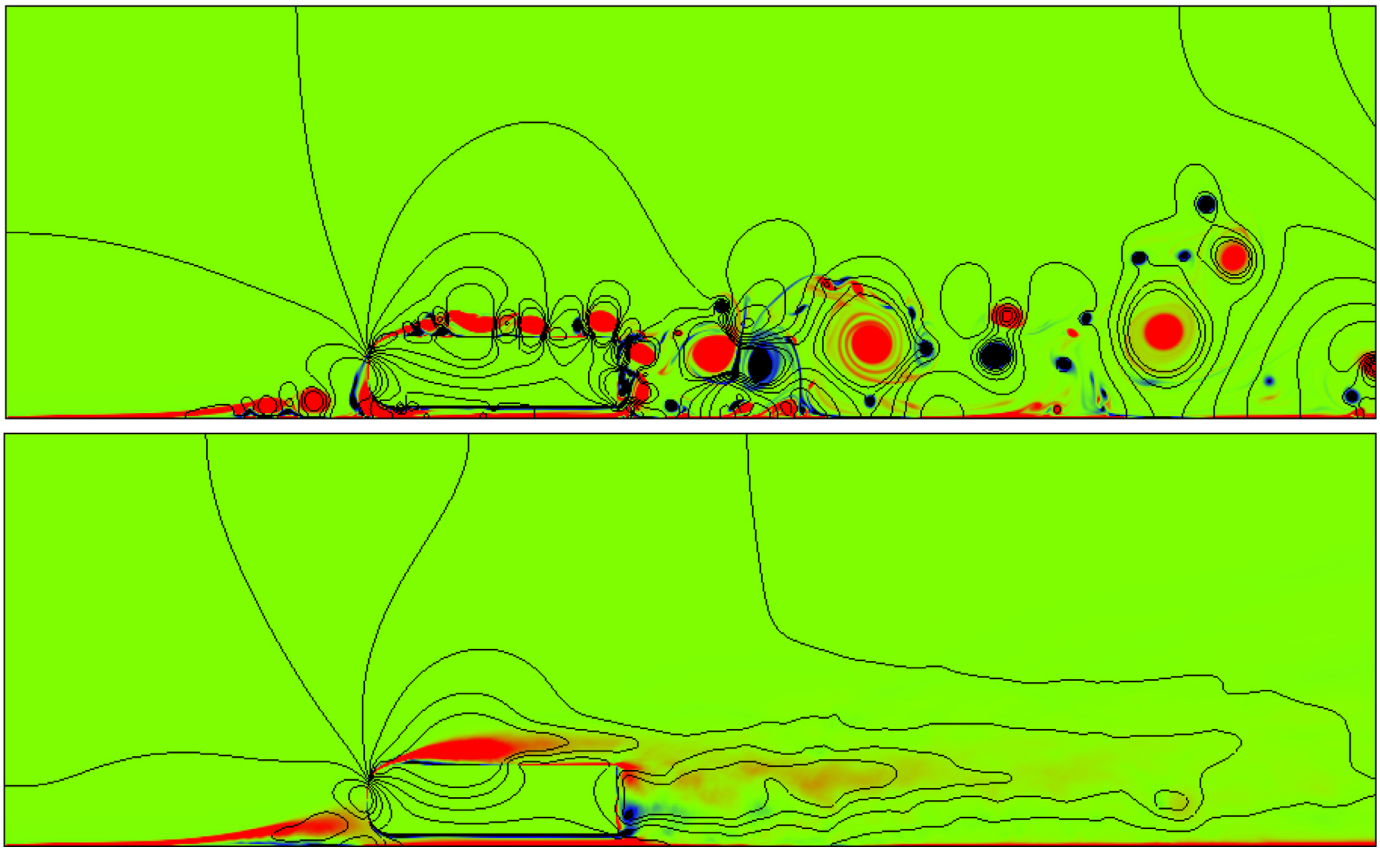

Fig. 1. Coloured vorticity field and pressure contours (black lines) of the flow over one single body on top of a road in two dimensions. Top: instantaneous flow, bottom: mean flow.

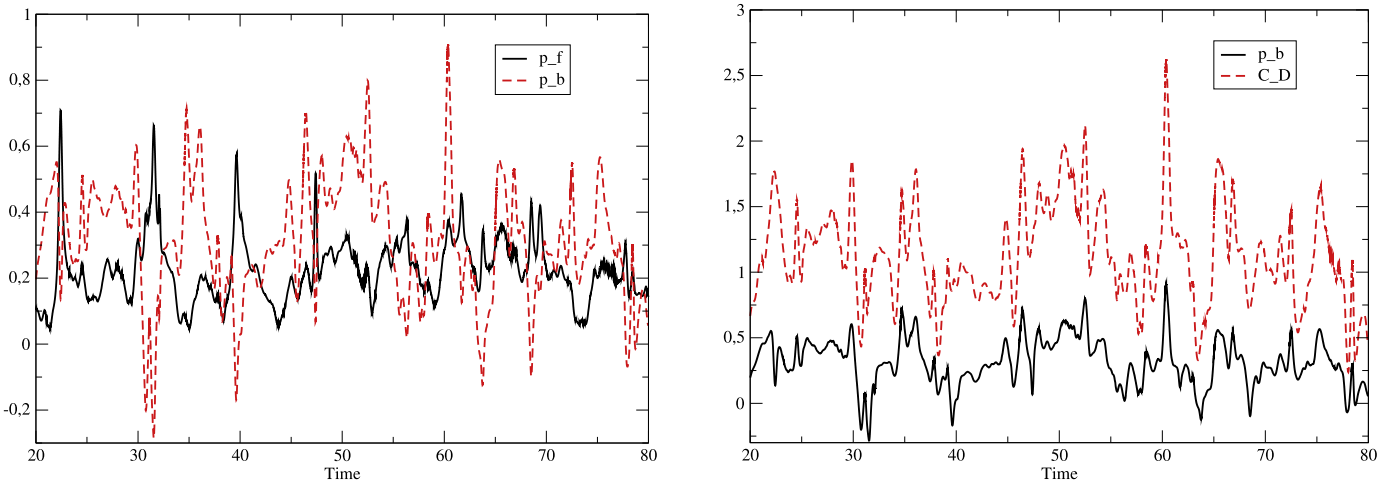

Fig. 2. Single body on top of a road in two dimensions: pressure forces p_f in front and p_b at the back (left) and strong correlation of the pressure at the back p_b and the drag coefficient C_D (right).

Table 2
Mean pressure forces and drag coefficient for one single body or two bodies on top of a road in two-dimensions. The variations are computed with respect to the single body.

Two-dimensions	p_f	variation	p_b	variation	C_D	variation
Single body	0.22		0.31		1.13	
First body $d = 0.2L$	0.24	+9%	−0.01	−103%	0.52	−64%
Second body $d = 0.2L$	0.024	−89%	0.25	−19%	0.58	−49%
First body $d = 0.5L$	0.24	+9%	0.16	−48%	0.85	−25%
Second body $d = 0.5L$	−0.09	−141%	0.2	−35%	0.24	−79%
First body $d = L$	0.3	+36%	0.15	−52%	0.96	−15%
Second body $d = L$	−0.03	−114%	0.25	−19%	0.48	−58%

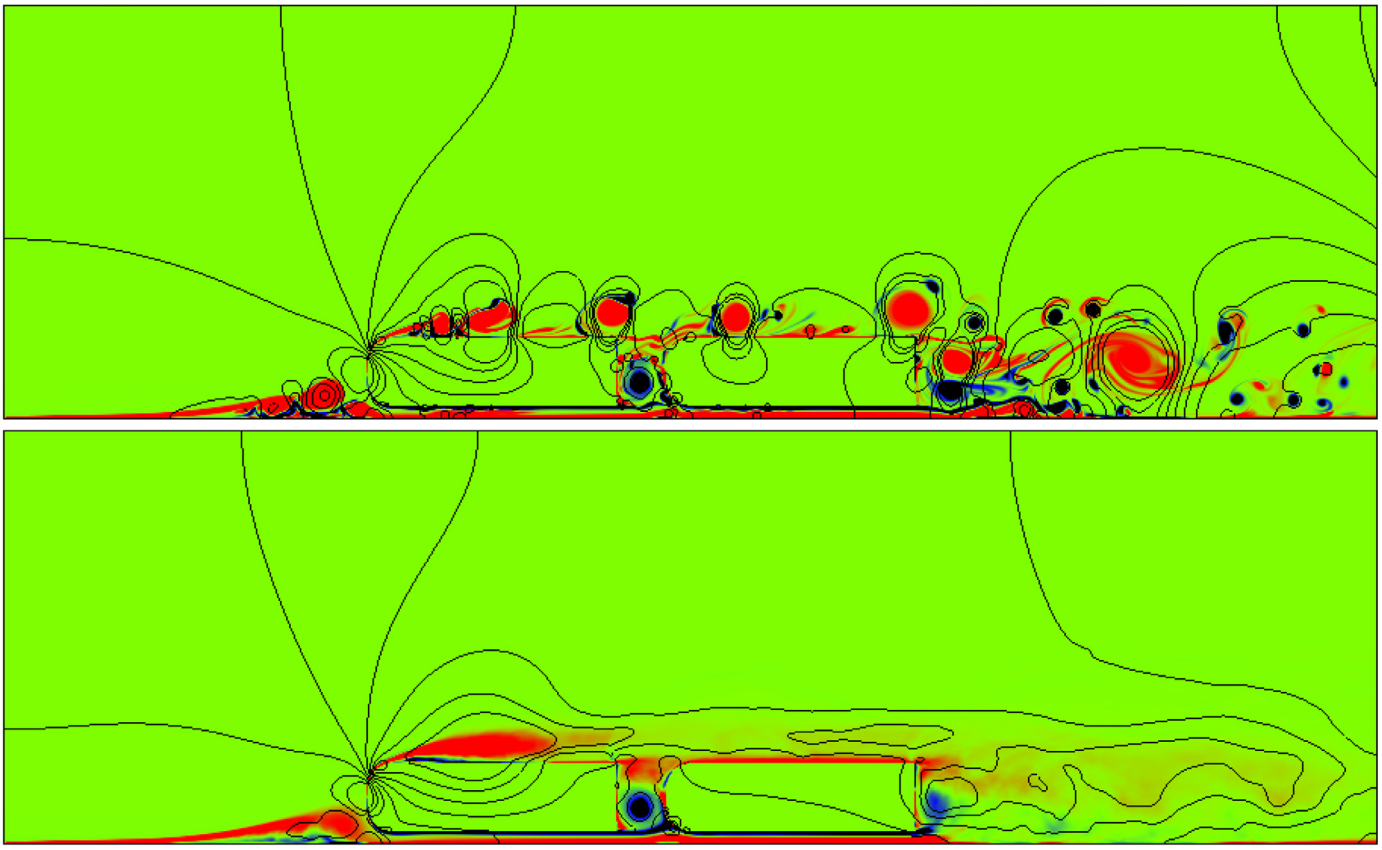

Fig. 3. Coloured vorticity field and pressure contours (black lines) of the flow over two bodies with $d = 0.2L$ on top of a road in two dimensions. Top: instantaneous flow, bottom: mean flow.

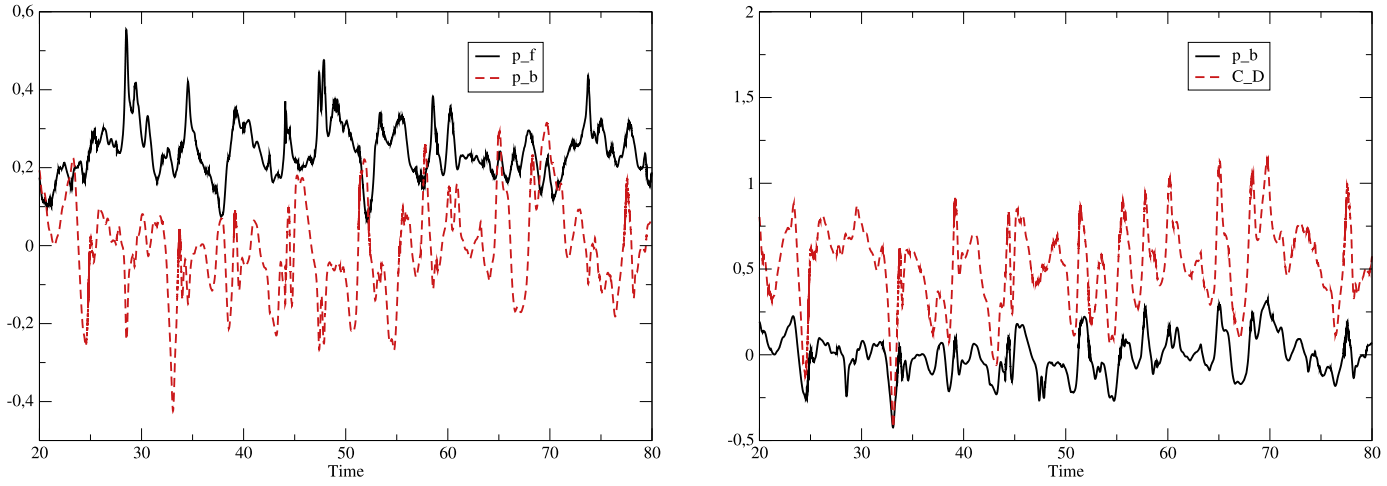

Fig. 4. Two bodies with $d = 0.2L$ on top of a road in two dimensions: pressure forces p_f in front and p_b at the back of the first body (left) and strong correlation of the pressure at the back p_b and the drag coefficient C_D (right).

of the drag coefficient by 79%. As for $d = 0.2L$ the drag coefficient of the first body is correlated to the pressure force at the back and the drag coefficient of the second body is correlated to the pressure force in front as shown in Fig. 7.

For the distance $d = L$ the flow is fully developed between the two bodies as shown in Fig. 8. In the two previous cases, the pressure in front of the first body slightly increases but for this new distance the increase is more significant. Thus the gain in the drag coefficient is only 15% (see Table 2). For the second body the behaviours are similar than for $d = 0.5L$ but weaker and so the reduction is weaker but still high with 58%. Once again the drag coefficient of the first body is correlated to the pressure force at the back and the drag coefficient of the second body is correlated to the pressure force in front as shown in Fig. 9. The analysis reported here is close to what was observed in Martinuzzi and Havel (2000).

3.2. Platooning on top of a road in three dimensions

In this section we explore the flow around one single, two or three Ahmed bodies following each other on top of a road in three dimensions. The simulations are performed on a 2, 560 × 768 ×

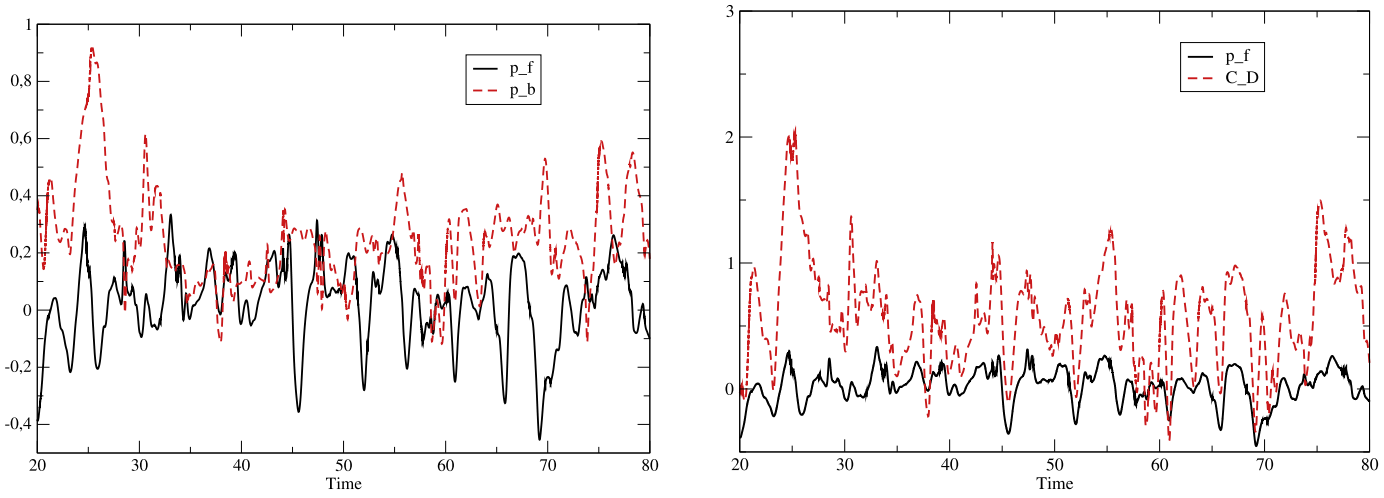

Fig. 5. Two bodies with $d = 0.2L$ on top of a road in two dimensions: pressure forces p_f in front and p_b at the back of the second body (left) and strong correlation of the pressure in front p_f and the drag coefficient C_D (right).

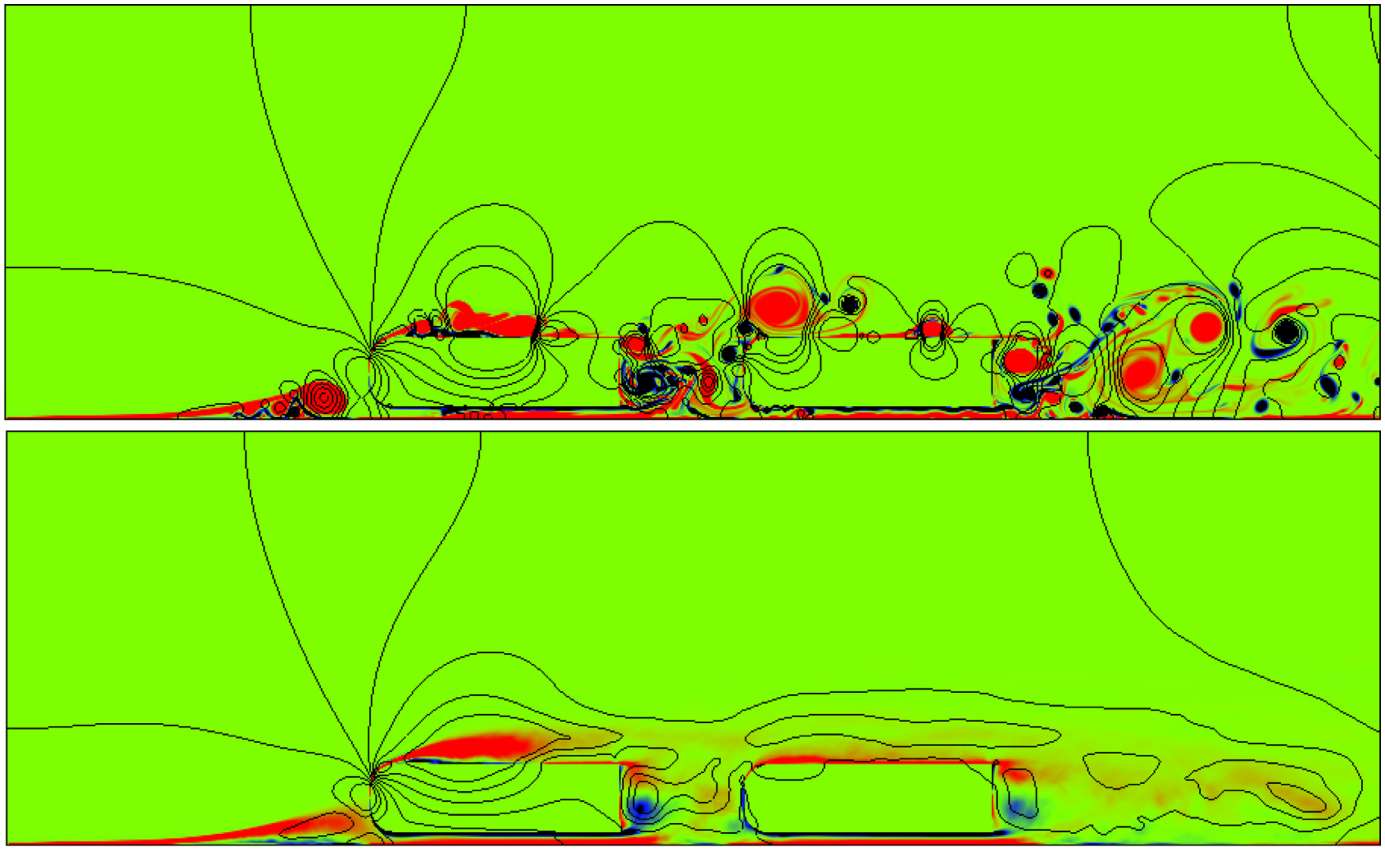

Fig. 6. Coloured vorticity field and pressure contours (black lines) of the flow over two bodies with $d = 0.5L$ on top of a road in two dimensions. Top: instantaneous flow, bottom: mean flow.

768 grid at Reynolds number $Re = 15,000$. The bodies are centered in the span wise direction.

Fig. 10 shows the pressure contours of the mean flow around the single body. Throughout the paper the blue contours reveal low pressures and the red contours high pressures. There are a high pressure zone in front and a low pressure zone at the back that have a crucial influence on the drag coefficient as both slow down the vehicle. In Fig. 11 the vorticity field and the pressure contours in the mid plane for one single body are represented. It shows that the wake is shorter than in two dimensions due to the size of the vortical structures but there is still a significant pressure well behind the body. Consequently, both pressure forces p_f and p_b are strong and responsible of 81% of the drag coefficient and thus the frictional drag is less than 20%. The pressure force at the back is about 1.5 larger than the pressure force in the front and the drag coefficient fluctuates with the pressure force at the back as in two dimensions (see Fig. 12). The mean drag coefficient obtained for one single body in a large domain and a long simulation time is $C_D = 0.455$ (Table 3) that is a little bit different from the value obtained for the grid convergence. This is due to the fact that in

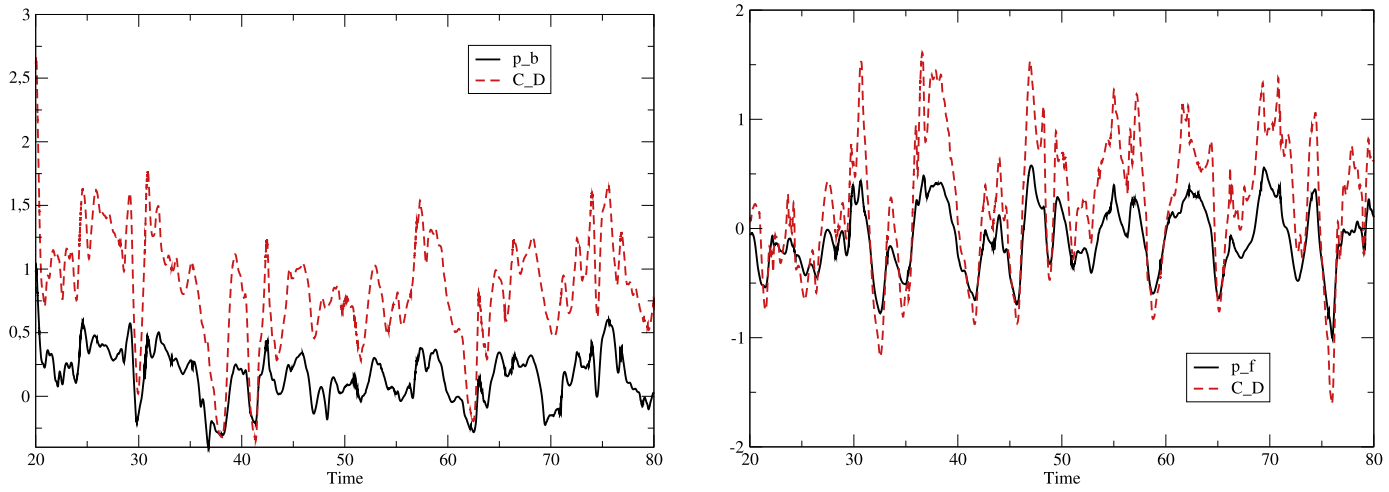

Fig. 7. Two bodies with $d = 0.5L$ on top of a road in two dimensions: pressure force p_b at the back and drag coefficient C_D of the first body (left) and pressure force p_f in front and drag coefficient C_D of the second body (right). Strong correlation is seen in both cases.

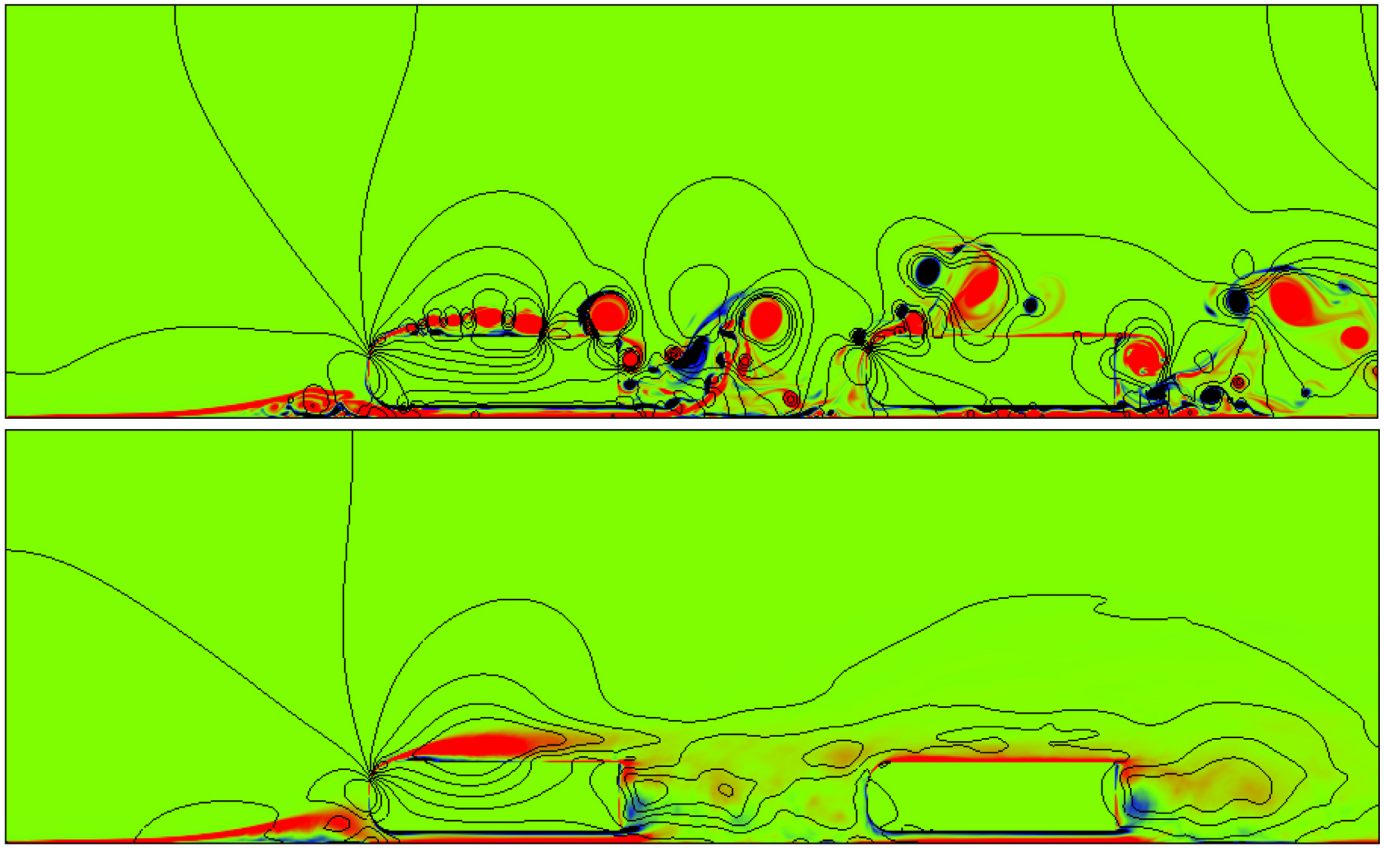

Fig. 8. Coloured vorticity field and pressure contours (black lines) of the flow over two bodies with $d = L$ on top of a road in two dimensions. Top: instantaneous flow, bottom: mean flow.

Table 3
Mean pressure forces and drag coefficient for one single body or two bodies on top of a road in three-dimensions. The variations are computed with respect to the single body.

Three-dimensions	p_f	variation	p_b	variation	C_D	variation
Single body	0.1		0.15		0.455	
First body $d = 0.2L$	0.11	+10%	0.05	−67%	0.31	−32%
Second body $d = 0.2L$	0.006	−94%	0.14	−7%	0.29	−36%
First body $d = 0.5L$	0.11	+10%	0.05	−67%	0.32	−30%
Second body $d = 0.5L$	0.1		0.13	−13%	0.41	−10%
First body $d = L$	0.11	+10%	0.11	−27%	0.41	−10%
Second body $d = L$	0.07	−30%	0.13	−13%	0.37	−19%

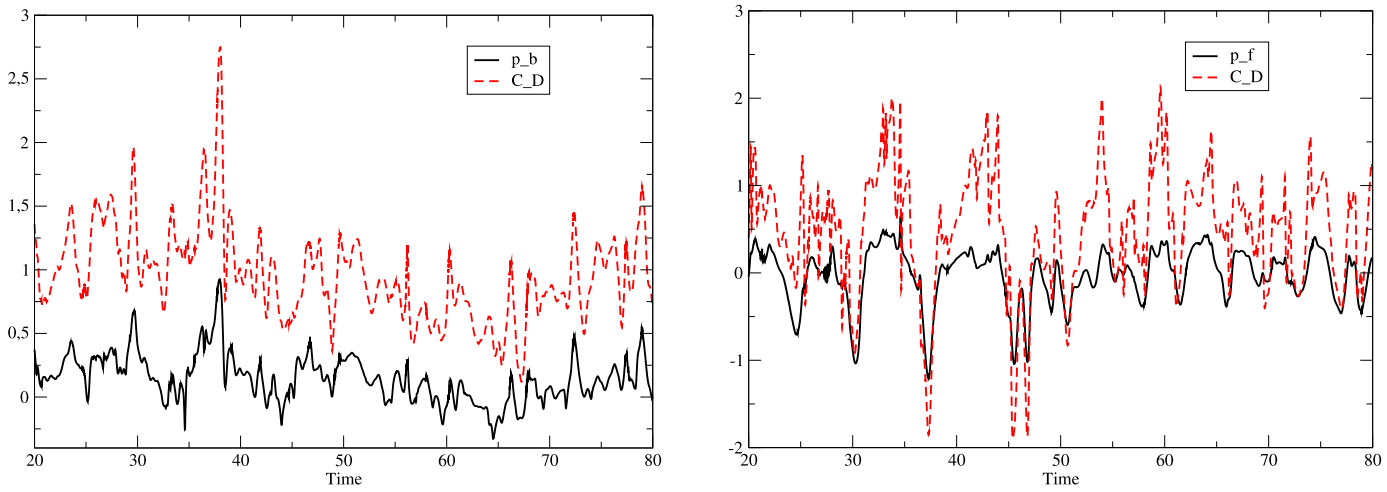

Fig. 9. Two bodies with $d = L$ on top of a road in two dimensions: pressure force p_b at the back and drag coefficient C_D of the first body (left) and pressure force p_f in front and drag coefficient C_D of the second body (right). Strong correlation is seen in both cases.

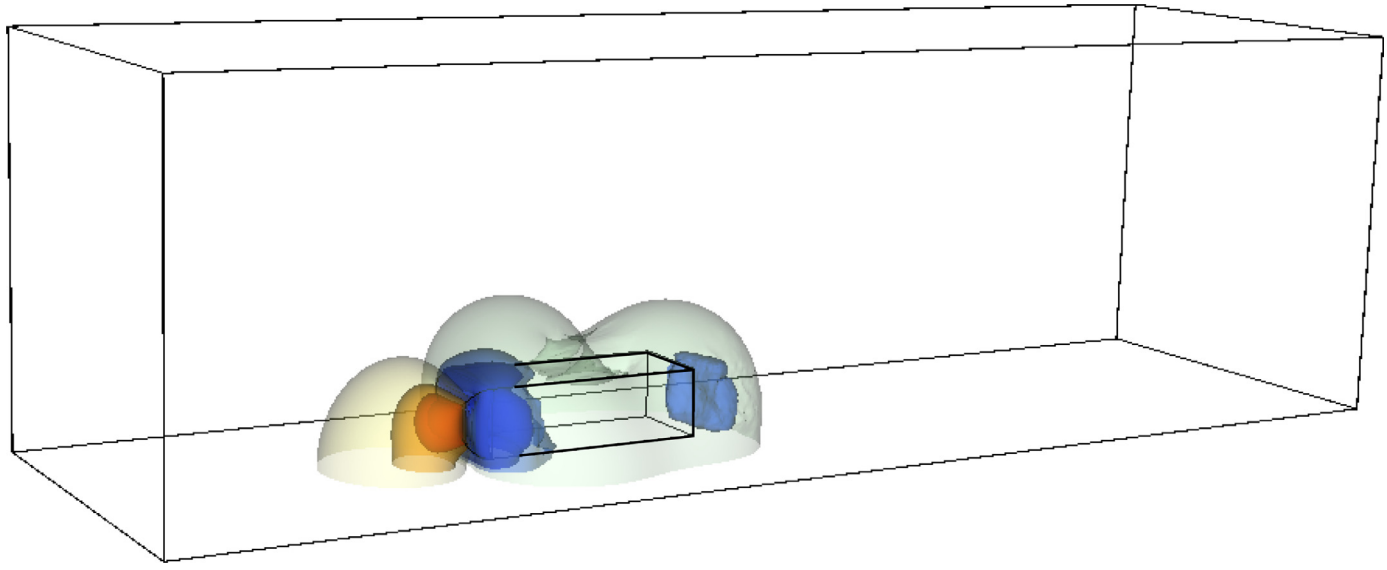

Fig. 10. Pressure contours of the mean flow around the single body in three dimensions. The dark colors show the high absolute values.

the short domain used for the grid convergence the exit section is close to the back of the body and thus can induce a small change in the pressure field. Moreover the simulation time is shorter for the grid convergence study. So the mean value is less reliable than in this section. This value of the mean drag coefficient will be the reference value for comparison to other simulations in a large domain with two or three bodies. For all the following simulations we keep the same level of grid and the same simulation time. In addition the mean flow is always computed on the same time interval taking the mean of 40,000 solutions.

The next simulations concern two bodies following each other with a distance $d = 0.2L$, $d = 0.5L$ or $d = L$ as in two dimensions. In Fig. 13 there is no high or low pressure zone between the two bodies that are so close that they almost behave like a long single body. Fig. 14 shows the vorticity field and the pressure contours in the mid plane. We notice that the presence of the second body inhibits the wake of the first body, reducing drastically the pressure force at the back of the first body and the pressure force in front of the second body. Consequently there is a strong reduction (more than 30%) of the drag coefficient of both bodies (Table 3).

When the distance is increased to $d = 0.5L$ the situation is different as the wake can be developed inside the gap between the two vehicles but there is still a strong compression at the back of the first body (see Figs. 16 and 17). Thus the pressure force at the back of the first body remains very low whereas the pressure force in front of the second body increases significantly. As a consequence the drag coefficient of the first body is still reduced by 30% but the drag coefficient of the second body is only reduced by 10% as shown in Table 3. Finally for $d = L$ the wake of the first body is almost fully developed as can be seen in Fig. 18. Thus the pressure force at the back is high and the reduction of the drag coefficient is only 10% (see Fig. 19 and Table 3). This time the pressure force in front of the second body is lower and the reduction of the drag coefficient for this body is 19%. (Fig. 15).

On the other hand we can notice in Table 3 that the pressure force in front of the first body is always the same whatever the distance d is. It is 10% higher than those of the single body. This is probably due to the apparent length of the convoy that is larger than the length of a single body. Similarly the pressure force at the back of the second body is also about the same and is about 10% lower than those of the single body. So the reduction of the drag

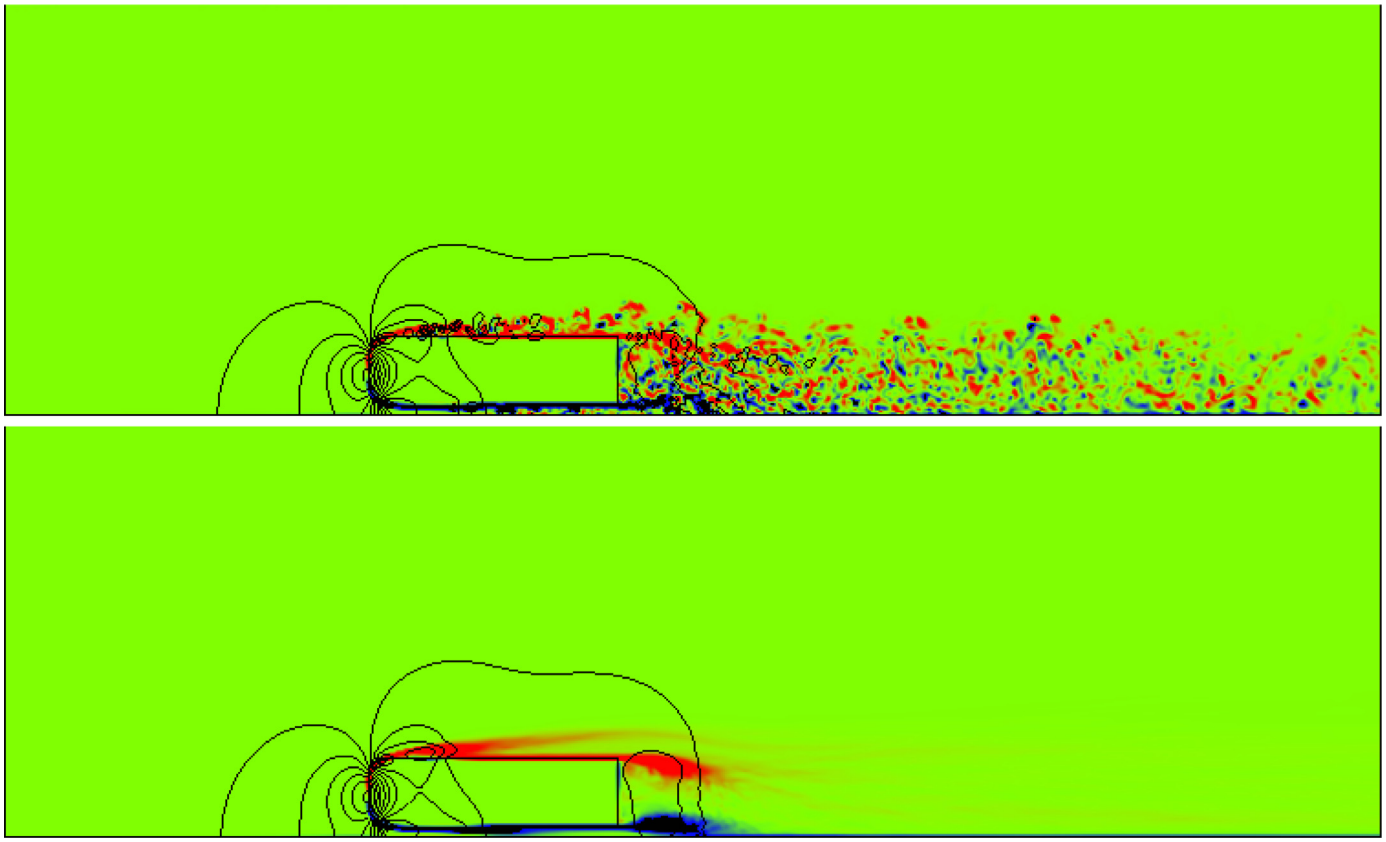

Fig. 11. Coloured Y-vorticity field and pressure contours (black lines) of the flow over one single body on top of a road in the mid plane in three dimensions. Top: instantaneous flow, bottom: mean flow.

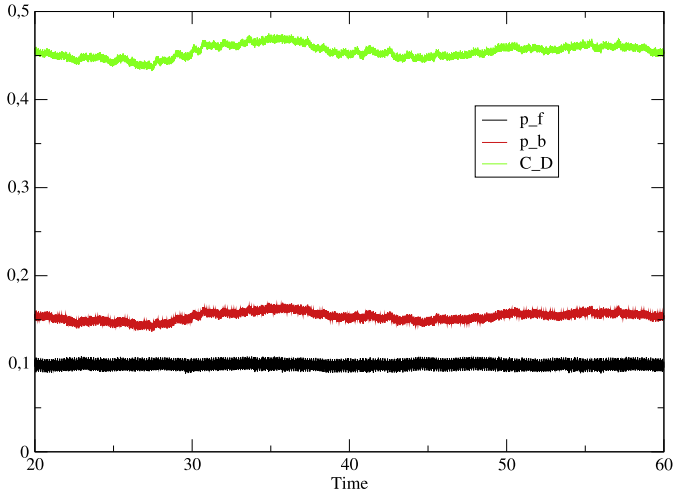

Fig. 12. Pressure forces p_f in front and p_b at the back and drag coefficient C_D of the single body in three dimensions.

coefficient is strongly linked to the flow behaviour inside the gap between the vehicles as we have already seen in two dimensions. In Fig. 20 is plotted the Y-vorticity contours for the instantaneous and mean flows showing almost the same behaviour for both bodies. That means that for a longer distance as $d = 2L = 7.25H$ for instance the flow around the two bodies would behave like the flow around two separate single bodies and there is no platooning any more. In a previous study (Bruneau et al., 2013) we have seen that there is still a positive effect for $d = 5H$, but beyond there is no more link between the two vehicles. So the inter vehicular communications must be able to handle quite short distances to have an efficient platooning.

To conclude this section we propose a new set of simulations involving three bodies to really quantify the platooning effect with a vehicle neither in front nor in queue. These simulations are performed on an extended domain $\Omega = (0, 24H) \times (0, 6H) \times (0, 6H)$ for $d = 0.2L$ and $d = 0.5L$ and $\Omega = (0, 24H) \times (0, 6H) \times (0, 6H)$ for $d = L$. To present the results we focus on the case $d = 0.5L = 1.8125H$, that means that for a truck of height about 4 meters, the distance between the trucks is about 7 meters. Which is a quite close distance actually. For this distance the flow inside the two gaps between the vehicles shown in Figs. 21 and 22 is very similar. So this is a situation that seems very stable and gives a strong sense of platooning. The result is quite surprising as the drag reduction is better than for the two bodies case. Indeed the drag reduction is now 34% for the two first bodies instead of 30% and the drag reduction is 25% for the last body instead of 10% (see Table 4). This result shows the real efficiency of platooning that can induce a drastic reduction of the fuel consumption. The same computations have been performed for the two other distances and the results are gathered in Table 5. They show about the same drag reduction than in the two bodies case for the first body but again the results are better for the other bodies. Even for $d = L = 3.625H$ there is a significant gain of the order 25%. This distance, although much less than the security distance, is probably more realistic as for a truck of 4 meters high it corresponds to 15 meters.

4. Numerical results with a simplified truck

To conclude this study, the flow around a more realistic body is computed. Indeed, the purpose of this work is to see how trucks can take benefit of platooning but the Ahmed body is quite far

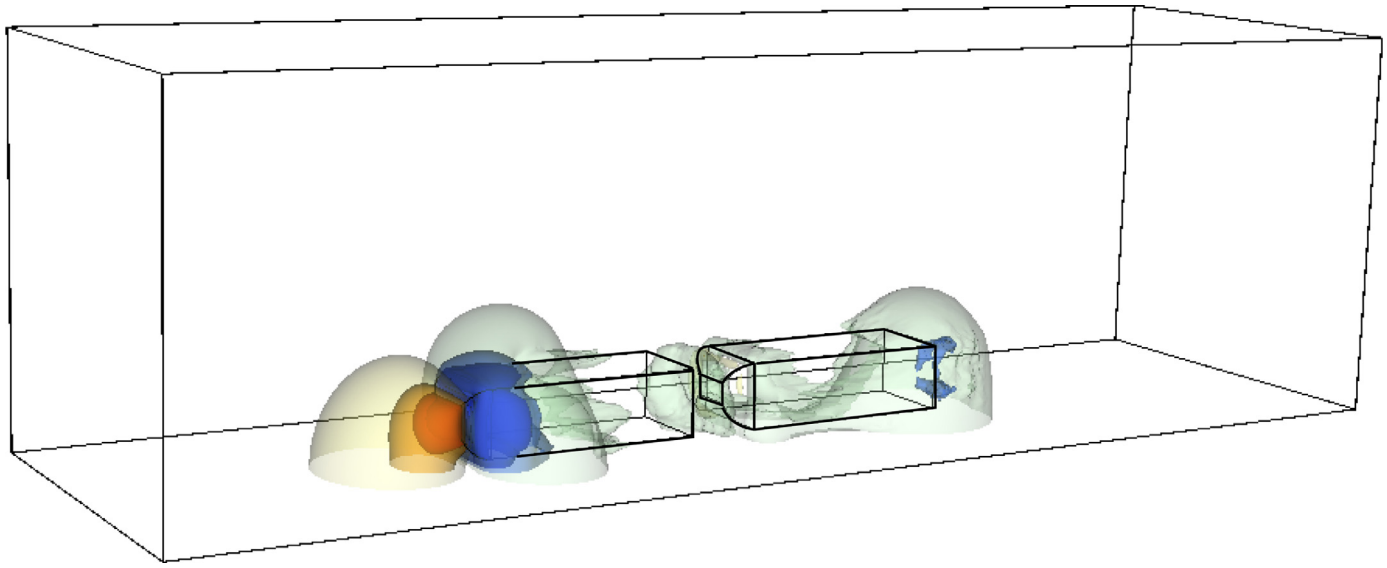

Fig. 13. Pressure contours of the mean flow around two bodies with $d = 0.2L$ in three dimensions. The dark colors show the high absolute values.

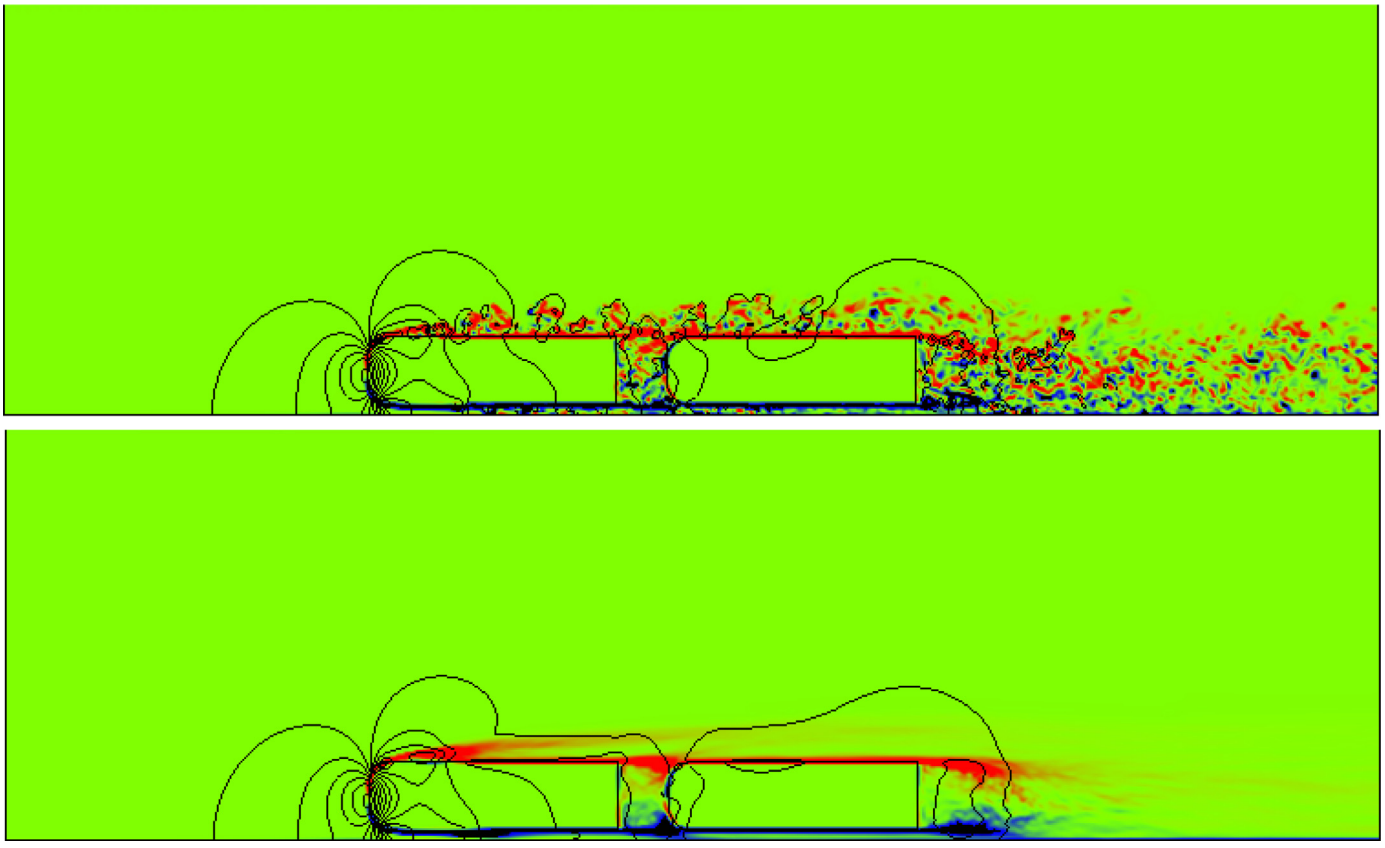

Fig. 14. Coloured Y-vorticity field and pressure contours (black lines) of the flow over two bodies with $d = 0.2L$ on top of a road in the mid plane in three dimensions. Top: instantaneous flow, bottom: mean flow.

Table 4
Mean pressure forces and drag coefficient for two or three bodies on top of a road in three-dimensions with $d = 0.5L$. The variations are computed with respect to the first of the two bodies and the last column is the variation with respect to the single body.

Three-dimensions	p_f	variation	p_b	variation	C_D	variation	single body variation
Single body	0.1		0.15		0.455		
First of two bodies	0.11		0.05		0.32		−30%
Second of two bodies	0.1	−9%	0.13	+160%	0.41	+28%	−10%
First of three bodies	0.12	+9%	0.03	−60%	0.3	−6%	−34%
Second of three bodies	0.11		0.05		0.3	−6%	−34%
Third of three bodies	0.06	−45%	0.12	+140%	0.34	+6%	−25%

Table 5
Mean pressure forces and drag coefficient for three bodies on top of a road in three-dimensions with $d = 0.2L$, $d = 0.5L$ and $d = L$. The variations are computed with respect to the single body.

Three-dimensions	p_f	variation	p_b	variation	C_D	variation
Single body	0.1		0.15		0.455	
First body $d = 0.2L$	0.11	+10%	0.05	−67%	0.31	−32%
Second body $d = 0.2L$	0.015	−85%	0.05	−67%	0.17	−63%
Third body $d = 0.2L$	−0.004	−104%	0.12	−20%	0.24	−47%
First body $d = 0.5L$	0.12	+20%	0.03	−80%	0.3	−34%
Second body $d = 0.5L$	0.11	+10%	0.05	−67%	0.3	−34%
Third body $d = 0.5L$	0.06	−40%	0.12	−20%	0.34	−25%
First body $d = L$	0.12	+20%	0.1	−33%	0.4	−12%
Second body $d = L$	0.08	−20%	0.1	−33%	0.33	−27%
Third body $d = L$	0.06	−40%	0.13	−13%	0.35	−23%

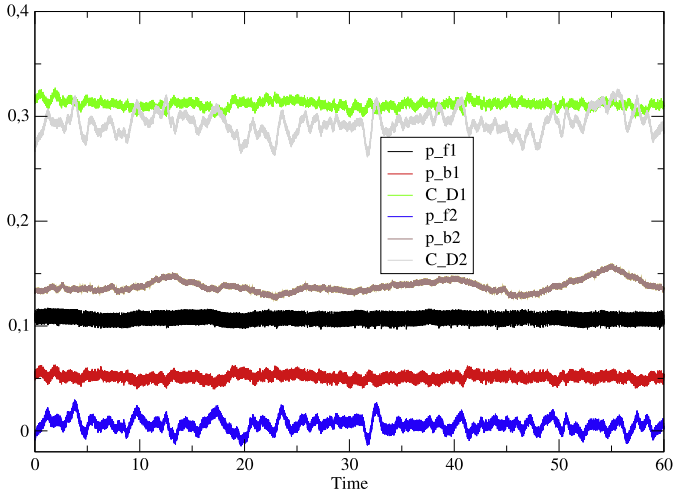

Fig. 15. Pressure forces p_f in front and p_b at the back and drag coefficient C_D of the two bodies with $d = 0.2L$ in three dimensions.

from a truck. So a simplified European tractor-trailer geometry (SETTG) is proposed to see the influence of the trailer on the whole flow and to quantify the gain due to platooning for such a geometry more similar to real trucks. This simplified tractor is close in sizes to European tractors with a rounded shape (with radius R) on top and both sides of the front of the tractor but not at the bottom as shown on the profile plotted in Fig. 23. It is lower than the trailer and the gap between the tractor and the trailer is small as usual. The trailer has a large length 4.7 times its height and a width 0.74 times its height. All the sizes of the SETTG are given in Fig. 23. As in the previous sections, the Reynolds number is related to the height of the body, here the height $H2$ of the trailer. Thus using the same Reynolds number than before $Re = 15,000$ corresponds to a very low speed.

The first numerical test concerns the flow around one single SETTG in a domain $\Omega = (0, 16H2) \times (0, 6H2) \times (0, 6H2)$ with the same level of grid than in the previous section and significant simulation times to have a good mean flow. The first observation is that, due to the total length of the body, the front and the back flows are not strongly linked like for the Ahmed body. Consequently there is a strong pressure force in front of the trailer (still denoted p_f) but the pressure force at the back of the trailer (still denoted p_b) is much reduced as shown in Fig. 24 and indicated in Table 6. For such a long body the viscous force is now of the same size than the pressure force at the back. So, the pressure force in front represents 55% of the drag coefficient while the pressure force at the back and the viscous force count for a little bit more than 20% each. The drag coming from the gap between the tractor and the trailer is very low.

The last numerical simulation involves three SETTG in a platoon with the distance between each other $d = 1.8125H2$ that is proportionally the same distance than $d = 0.5L = 1.8125H$ for Ahmed

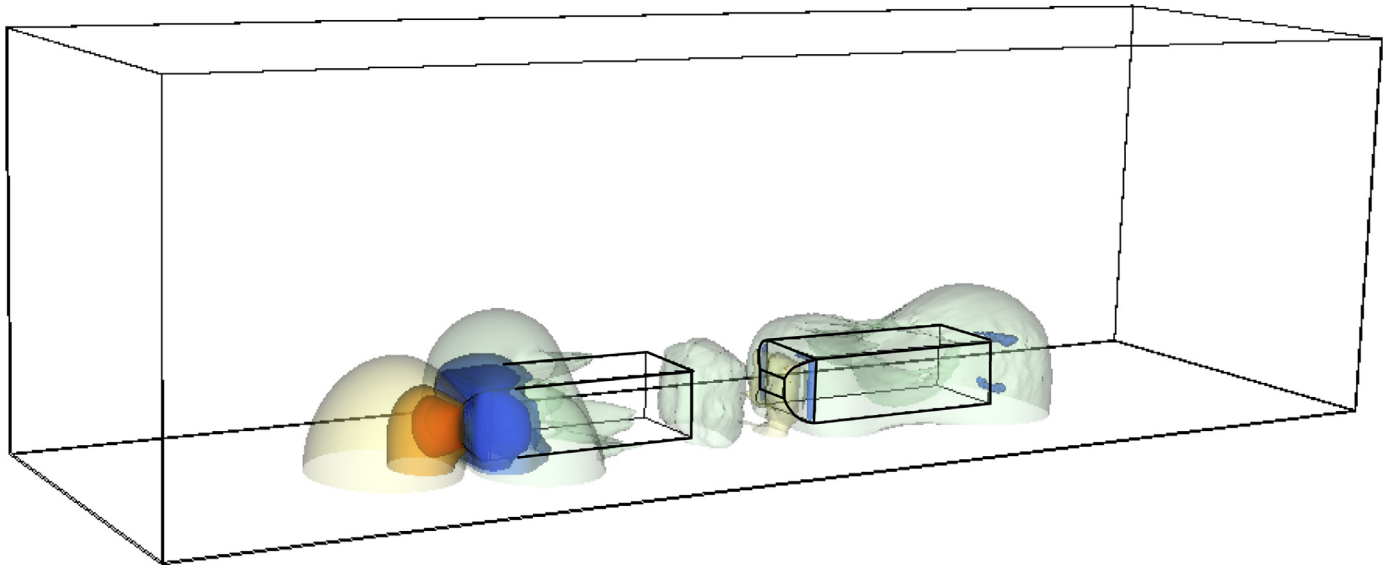

Fig. 16. Pressure contours of the mean flow around two bodies with $d = 0.5L$ in three dimensions. The dark colors show the high absolute values.

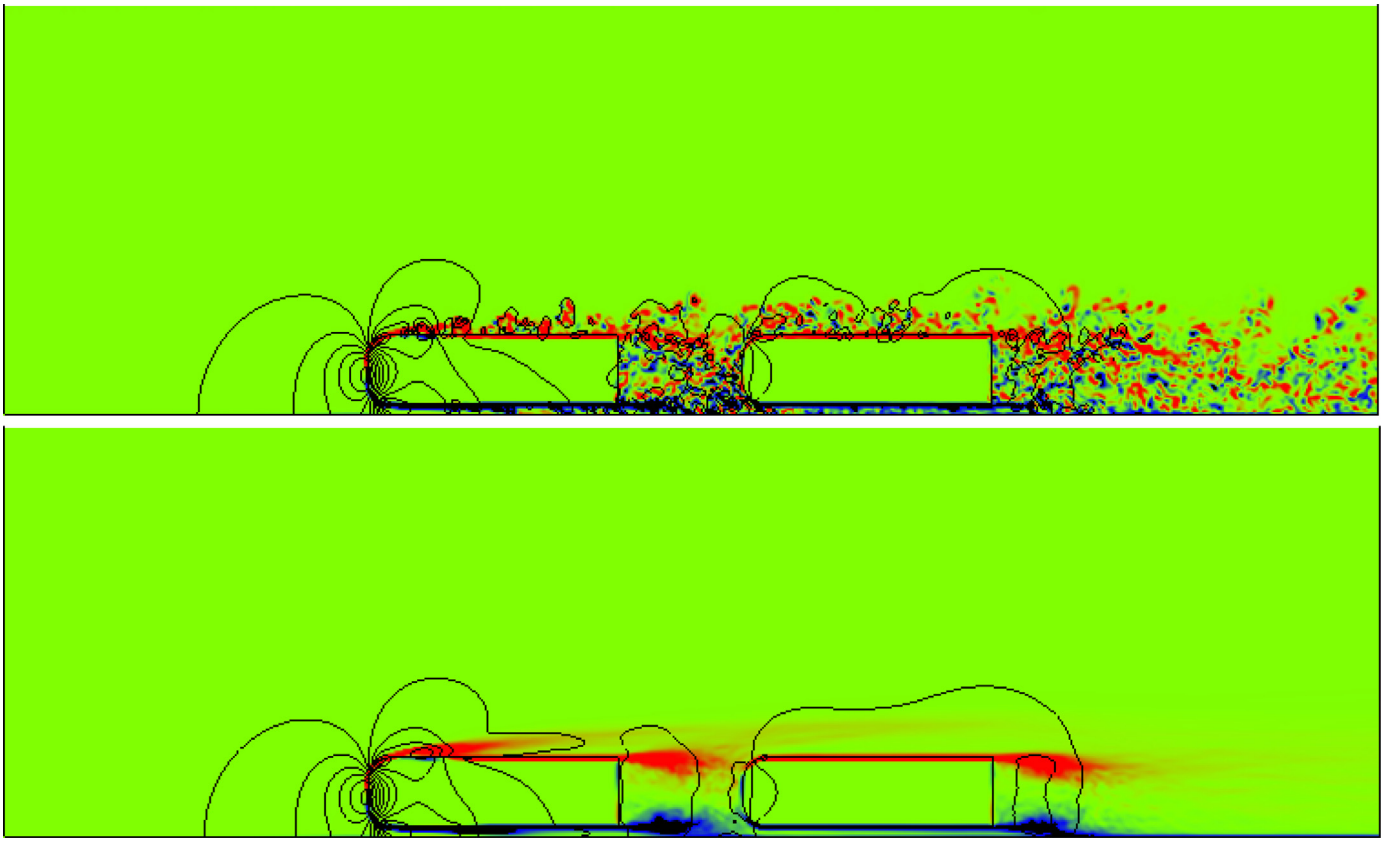

Fig. 17. Coloured Y-vorticity field and pressure contours (black lines) of the flow over two bodies with $d = 0.5L$ on top of a road in the mid plane in three dimensions. Top: instantaneous flow, bottom: mean flow.

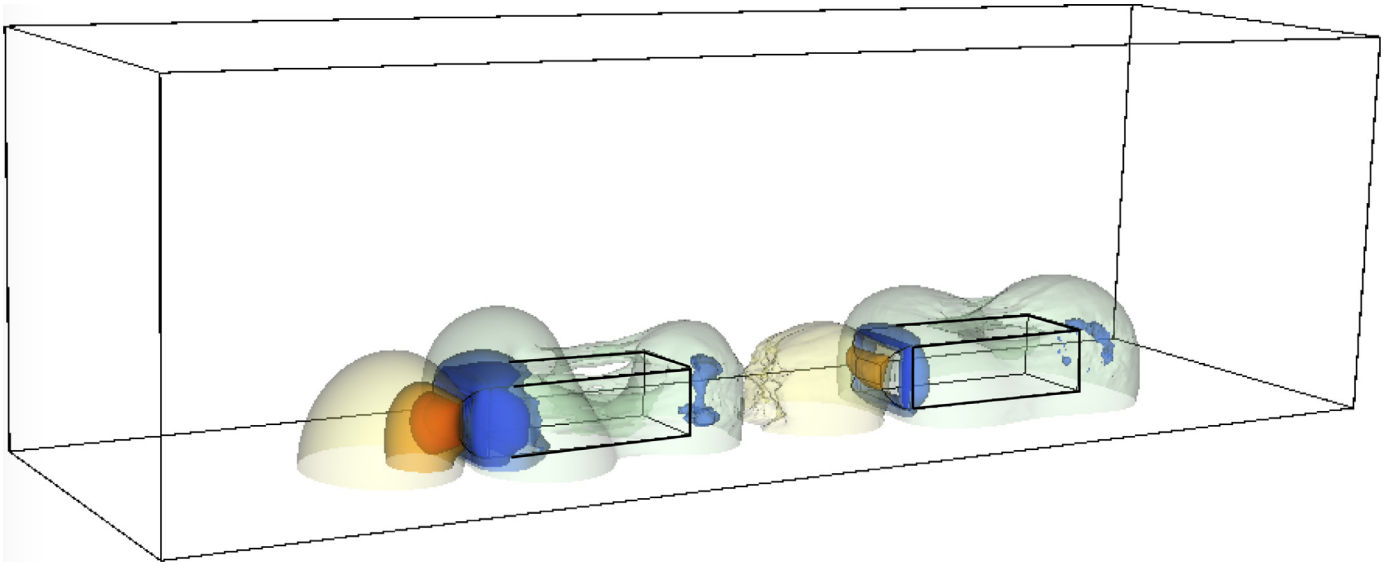

Fig. 18. Pressure contours of the mean flow around two bodies with $d = L$ in three dimensions. The dark colors show the high absolute values.

Table 6
Mean pressure forces and drag coefficient for three trucks (SETTG) on top of a road in three-dimensions with $d = 1.8125H2$. The pressure force P_f is only in front of the tractor and the pressure force P_b is only at the back of the trailer. The variations are computed with respect to the single body.

Three-dimensions	p_f	variation	p_b	variation	C_D	Variation
Single truck	0.15		0.06		0.74	
First of three trucks	0.16	+7%	0.03	−50%	0.66	−11%
Second of three trucks	0.07	−53%	0.02	−67%	0.42	−43%
Third of three trucks	0.06	−60%	0.05	−17%	0.46	−38%

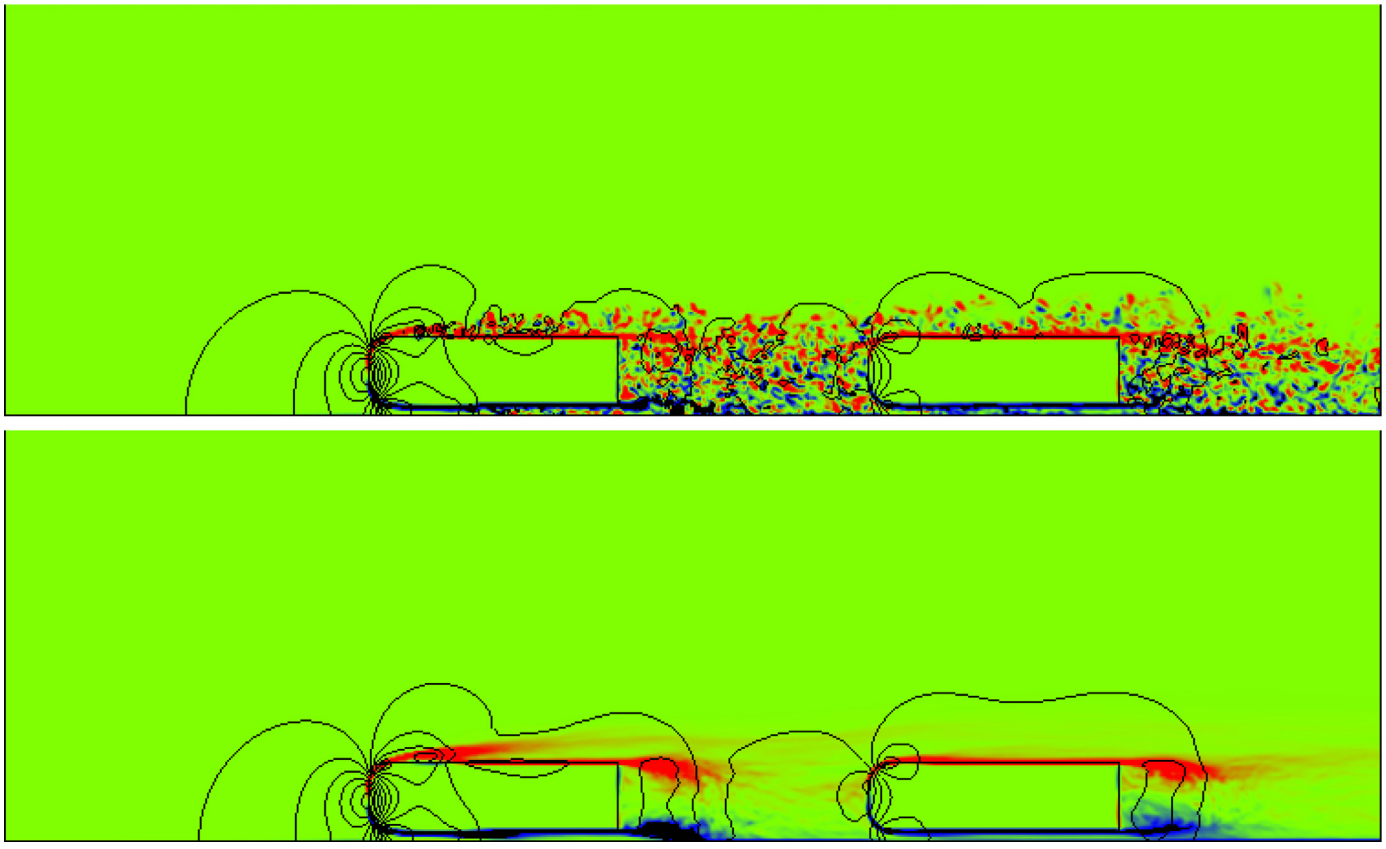

Fig. 19. Coloured Y-vorticity field and pressure contours (black lines) of the flow over two bodies with $d = L$ on top of a road in the mid plane in three dimensions. Top: instantaneous flow, bottom: mean flow.

bodies. The simulation is performed with the same approximation than before but on a larger domain $\Omega = (0, 28H2) \times (0, 6H2) \times (0, 6H2)$. In Fig. 25 it can be seen clearly that the following body compresses slightly the pressure well at the back of the preceding body. It appears that the pressure forces of the body in the middle are very low and consequently a 43% reduction of the drag coefficient is achieved. As the influence of the pressure force at the back is weaker than for Ahmed body, on the one hand the third body reaches a 38% reduction of the drag coefficient but on the other hand the first body obtains only a 11% reduction. In fact the pressure force in front of the first body is slightly increased like for Ahmed body. All these data are gathered in Table 6.

Similar results have been obtained in Uystepruyst and Krajnović (2013) for four cuboids in a row at a distance $d = 0.4L$. In that paper experiments and LES numerical simulations show a small reduction around 10% of the drag coefficient for the leading cuboid compare to a single one. But a strong reduction of the drag coefficient (more than 60%) is achieved for the following ones and the reduction of the drag coefficient is a bit less strong for the last one. In Humphreys and Bevly (2016) the authors analyze a generic two trucks platoon and find, at short distance between the two trucks, a drag coefficient reduction of 10% to 20% for the first truck and between 30% and 40% for the second one. Finally in Watts (2015) the author finds for three American trucks in platoon with a twenty feet separation distance a drag reduction of 13%, 48% and 40% respectively at a typical highway speed of a tractor-trailer. Surprisingly, these last results are very close to what we find in this study whereas the geometry and the speed are very different.

5. Conclusions

In this work numerical simulations of the flow around one, two or three simplified square-back vehicles in a row have been performed. Results in two- and three-dimensions show the efficiency of the platooning that induces a significant reduction of the pressure forces and consequently the drag coefficient decreases. Indeed, if the distance between the vehicles is small enough, the vehicle in front plays the role of a buckler and the pressure force in front of the following vehicle decreases. Similarly, the following vehicle compresses the pressure well at the back and thus the pressure force at the back of the preceding vehicle also decreases. As the pressure forces are responsible of a large part of the drag, the decrease of the pressure forces implies a similar decrease of the drag coefficient.

The results for three Ahmed bodies give an higher drag reduction than for two Ahmed bodies as a drag reduction around 30% is reached. Besides the simulations around simplified European tractor-trailer geometries give even a better result with about 40% reduction of the drag coefficient except for the first simplified truck. Which is very encouraging for the application to truck trains on highways.

Let us point out that this study is restricted to square-back vehicles like trucks for which the surrounding flow is very different from the one around usual cars with a rear window at a critical slant angle. In that case authors have reported a significant enhancement of the drag coefficient of the rear vehicle for $d = 0.5L$ for instance (Mirzaei and Krajnović, 2016; Pagliarella, 2009; Watkins and Vino, 2008). This may be due to the longitudinal vortices that break on the following vehicle.

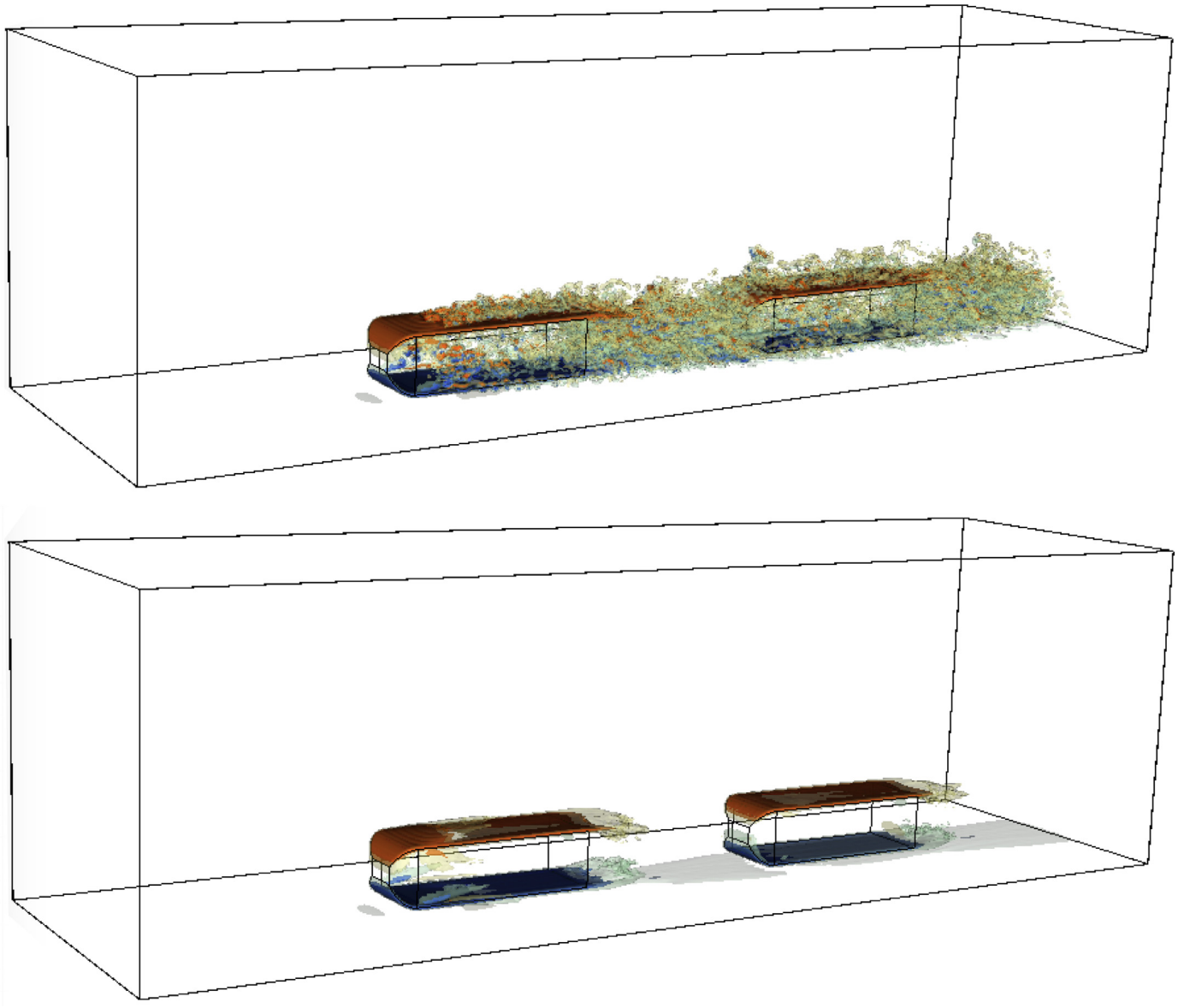

Fig. 20. Y-vorticity contours of the instantaneous (top) and mean (bottom) flow around two bodies with $d = L$ in three dimensions.

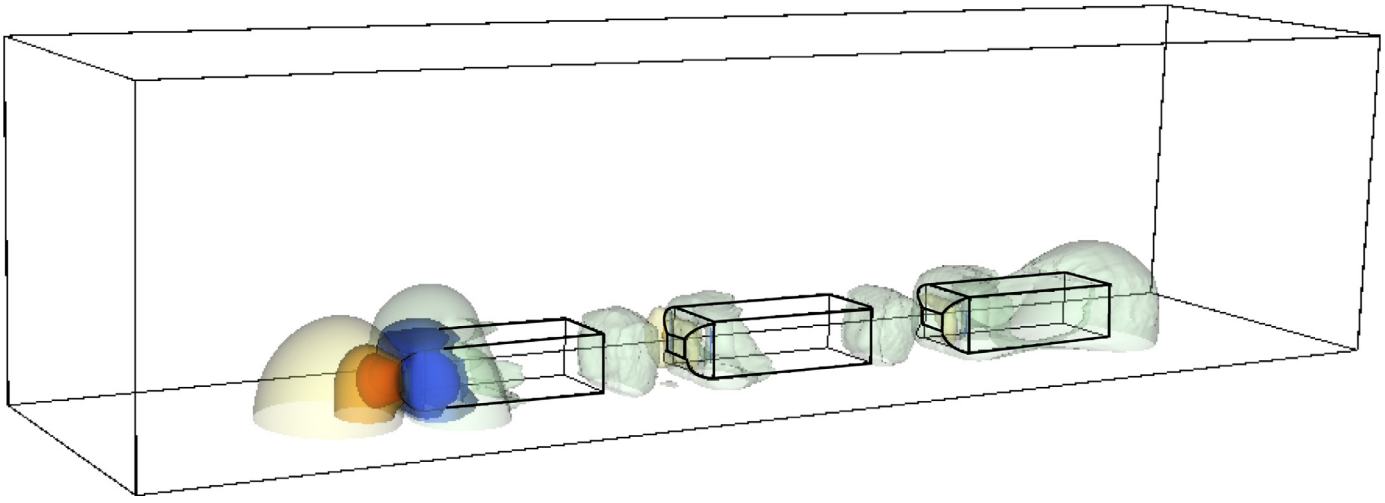

Fig. 21. Pressure contours of the mean flow around three bodies with $d = 0.5L$ in three dimensions. The dark colors show the high absolute values.

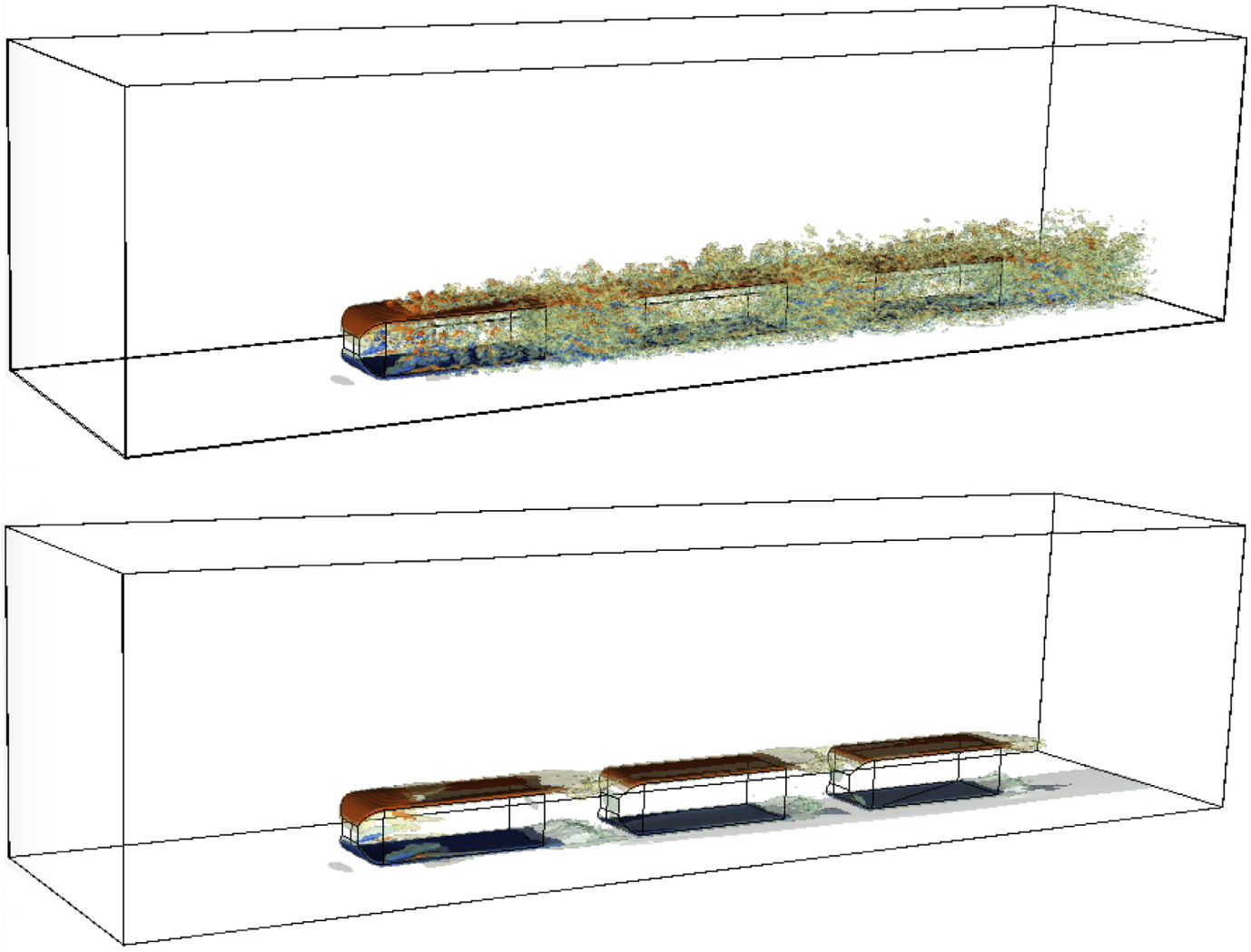

Fig. 22. Y-vorticity contours of the instantaneous (top) and mean (bottom) flow around three bodies with $d = 0.5L$ in three dimensions.

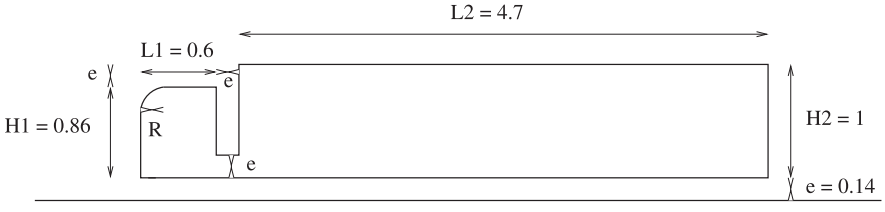

Fig. 23. Profile of the simplified European tractor-trailer geometry (SETTG) on top of a road. The sizes have no dimensions as they are related to the height of the trailer. The total length is $L = 5.44$, the width is $W = 0.74$ and the radius of the cylinders is $R = e = 0.14$.

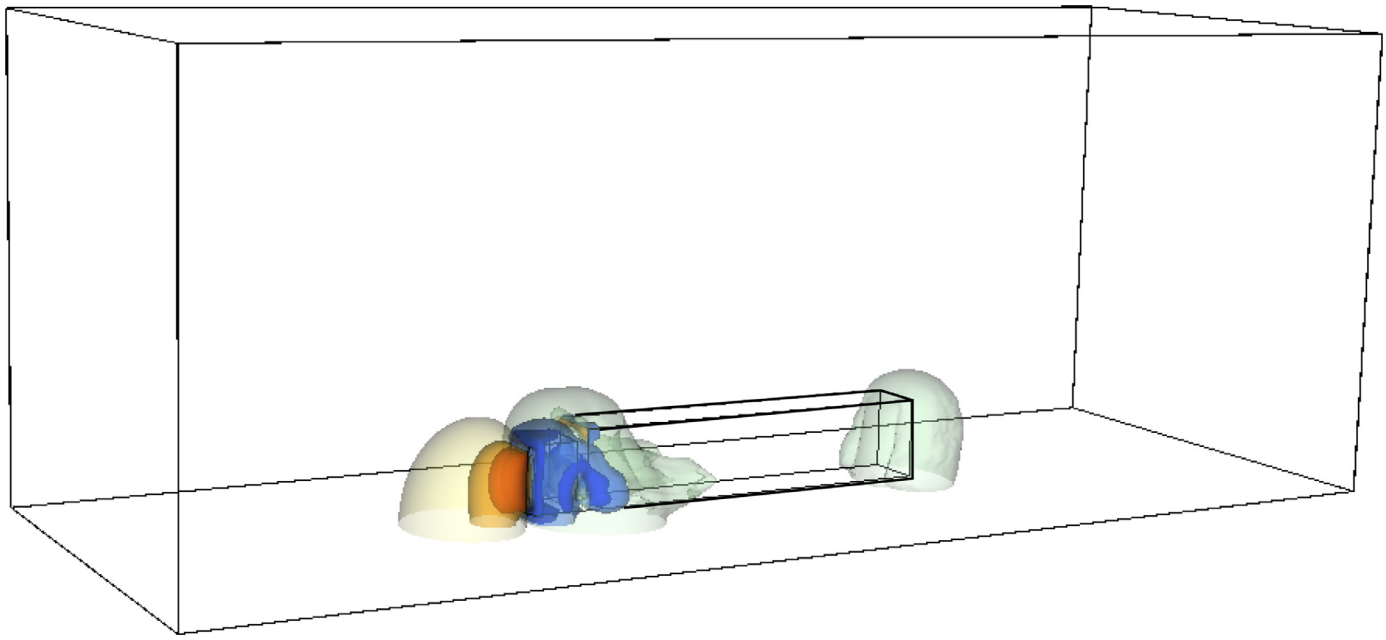

Fig. 24. Mean pressure contours of the mean flow around one single SETTG on top of a road in three dimensions. The dark colors show the high absolute values.

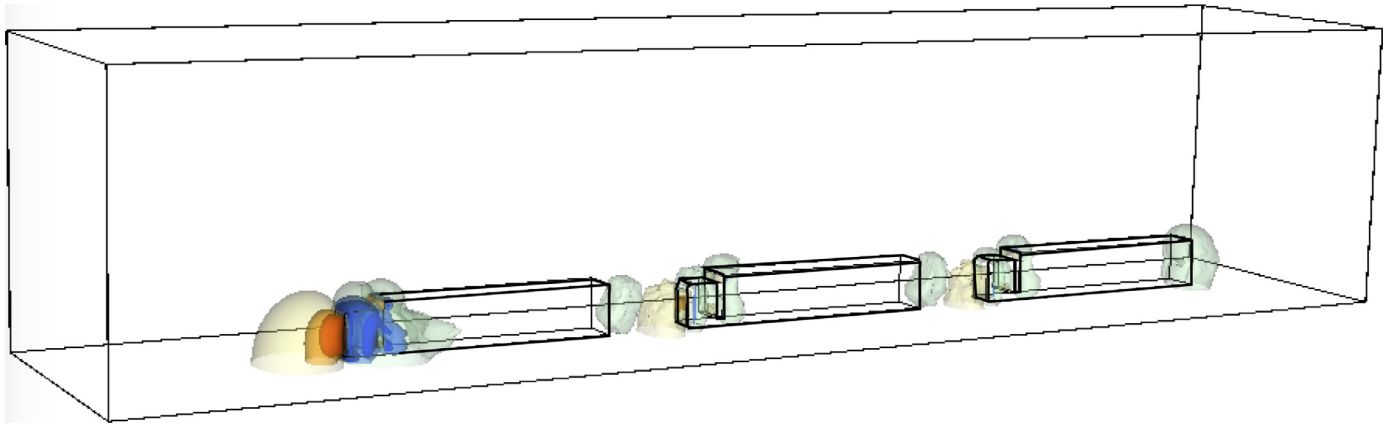

Fig. 25. Mean pressure contours of the mean flow around three SETTG with $d = 1.8125H2$ on top of a road in three dimensions. The dark colors show the high absolute values.

Acknowledgements

The numerical simulations presented in this paper have been run on PLAFRIM platform supported by IMB University of Bordeaux and INRIA Bordeaux - Sud Ouest.

References

Ahmed, S.R., Ramm, G., Faltin, G., 1984. Some salient features of the time-averaged ground vehicle wake. SAE-Paper. 840300.
Alam, A., Gattami, A., Johansson, K., 2010. An experimental study on the fuel reduction potential of heavy-duty vehicle platooning. In: Proceedings of the 13th International IEEE Annual Conference on Intelligent Transportation Systems.
Angot, P., Bruneau, C.-H., Fabrie, P., 1999. A penalization method to take into account obstacles in incompressible viscous flows. Numer. Math. 81.
van Arem, B., van Driel, C., R., V., 2006. The impact of cooperative adaptive cruise control on traffic-flow characteristics. IEEE Trans. Intell. Transp. Syst. 7 (4).
Bruneau, C.-H., 2000. Boundary conditions on artificial frontiers for incompressible and compressible Navier-Stokes equations. Math. Modell. Numer. Anal. 34 (2).
Bruneau, C.-H., Creusé, E., Gilliéron, P., Mortazavi, I., 2014. Effect of the vortex dynamics on the drag coefficient of a square back Ahmed body: application to the flow control. Eur. J. Mech. B/Fluids 45.
Bruneau, C.-H., Khadra, K., 2016. Highly parallel computing of a multigrid solver for 3d Navier-Stokes equations. J. Comput. Sci. 17 (1).
Bruneau, C.-H., Khadra, K., Mortazavi, I., 2013. Analysis and active control of the flow around two following Ahmed bodies. In: Proceedings FEDSM FEDSM2013-16588.
Bruneau, C.-H., Saad, M., 2006. The 2d lid-driven cavity problem revisited. Comput. Fluids 35 (3).
Brunn, A., Wassen, E., Sperber, D., Nitsche, W., Thiele, F., 2007. Active drag control for a generic car model, Active Flow Control. In: Notes on Numerical Fluid Mechanics and Multidisciplinary Design, 95. Springer, pp. 247–259.
Caltagirone, L., Torabi, S., Wahde, M., 2015. Truck platooning based on lead vehicle speed profile optimization and artificial physics. In: Proceedings IEEE International Conf.erence on Intelligent Transport Systems.
Farokhi, F., Johansson, K., 2014. Investigating the interaction between traffic flow and vehicle platooning using a congestion game. IFAC Proc. 19.
Frahadi, M., Sedighi, K., 2008. Flow over two tandem wall-mounted cubes using large eddy simulation. Proc. Inst. Mech. Eng. Part C 222.
Humphreys, L., Bevly, D., 2016. Computational fluid dynamic analysis of a generic 2 truck platoon. SAE Technical Paper. 2016-01-8008.
Kavathekar, P., Chen, Y., 2011. Vehicle platooning: a brief survey and categorization. In: ASME 2011 International Design Engineering Technical Conferences and Computers and Information in Engineering Conference.
Krajnović, S., Davidson, L., 2003. Numerical study of the flow around the bus-shaped body. ASME J. Fluids Eng. 125.
Martinuzzi, R., Havel, B., 2000. Turbulent flow around two interfering surface–mounted cubic obstacles in tandem arrangement. J. Fluids Eng. 122 (1).
Mirzaei, M., Krajnović, S., 2016. Large eddy simulations of flow around two generic vehicles in a platoon. In: Proceedings of the 5th International Conference on Jets, Wakes and Separated Flows.
Pagliarella, R., 2009. On the Aerodynamic Performance of Automotive Vehicle Pla-

toons Featuring Pre and Post-Critical Leading Forms. Ph.D. thesis. School of Aerospace, Mechanical and Manufacturing Engineering, RMIT University.
Pagliarella, R., Watkins, S., 2016. The effect of rear slant angle on vehicle wakes and implications for platoons. SAE Technical Paper. 2006-01-0341.
Segata, M., Bloessl, B., Joerer, S., Sommer, C., Gerla, M., Lo Cigno, R., Dressler, F., 2015. Toward communication strategies for platooning: simulative and experimental evaluation. IEEE Trans. Veh. Technol. 64 (12).
Sommer, C., Dressler, F., 2014. Vehicular Networking. Cambridge Univ. Press.
Uystepruyst, D., Krajnović, S., 2013. Les of the flow around several cuboids in a row. Int. J. Heat Fluid Flow 19, 414–424.
Watkins, S., Vino, G., 2008. The effect of vehicle spacing on the aerodynamics of a representative car shape. J. Wind Eng. Ind. Aerodyn. 96 (6).
Watts, A., 2015. Computational Characterization of Drag Reduction for Platooning Heavy Vehicles. Ph.D. thesis. Auburn Alabama USA.